R

Formation and application of porous silicon

H. Föll[*], M. Christophersen, J. Carstensen, G. Hasse
Faculty of Engineering, University of Kiel, Kaiserstrasse 2, D-24143 Kiel, Germany

Abstract

All manifestations of pores in silicon are reviewed and discussed with respect to possible applications. Particular emphasis is put on macropores, which are classified in detail and reviewed in the context of pore formation models. Applications of macro-, meso-, and micropores are discussed separately together with some consideration of specific experimental topics. A brief discussion of a stochastic model of Si electrochemistry that was found useful in guiding experimental design for specific pore formation concludes the paper.
© 2002 Elsevier Science B.V. All rights reserved.

Keywords: Electrochemistry; Microstructure; Self-organization; Porous silicon

1. Introduction

1.1. Scope and aim of the paper

The electrochemistry of Si (and of other semiconductors) exhibits a large range of peculiar phenomena, many of which are not well understood at present. The most prominent feature under anodic etching conditions is the formation of pores and ''porous silicon'' has attracted increasing interest for a wide spectrum of potential applications since the discovery of the unexpected optical properties of microporous Si in 1990 [1,2]. In this paper, we endeavor to cover applications of porous Si, and since there are several recent papers dealing with properties and applications of microporous Si [3–8], the focus of this paper will be on everything else, i.e. on mesoporous and macroporous Si.

The parameter space for pore formation is very large and has not been fully explored. As shown in recent papers [9–12], it is still possible to find new kinds of pores in Si with peculiar features that may be of interest for applications. We will therefore review and classify the many types of pores that have been observed.

The Si–electrolyte contact, however, has more to offer to science and technology than just pore formation. Specific features with potential uses include:

- ohmic or diode-type contacts with obvious potential for applications [13],
- interfaces with an extremely low density of interface states and therefore very low values of the surface recombination velocity [14–16],
- solar cell like behavior, i.e. photo currents which may increase linearly or non-linearly with the light intensity [17],

---

[*] Corresponding author. Tel.: +49-431-880-6175.
E-mail address: hf@tf.uni-kiel.de (H. Föll).

- anodic oxide formation in various modes [18],
- strong non-linear response to frequencies superimposed on voltages or currents as a relatively new issue [12–20],
- very peculiar anisotropies of certain properties, in particular macropore growth [21,22],
- self-induced current or voltage oscillations in certain areas of the parameter space for constant external voltage or current, respectively (referred to as potentiostatic or galvanostatic conditions), cf. [23,24].

All points, except the last two, have found applications (at least in proposals), and it is quite possible that new features will be added to this list in due time. So far, e.g. no self-ordered pore arrays have been observed as reported for Al_2O_3 [25] or, more to the point, for GaAs [26,27], GaP [28,29] or InP [30,31]—always occurring with self-induced voltage oscillations (cf. Fig. 29). Will we be able to find self-ordered pores in Si, too? Also in connection with voltage oscillations? If not—why not? Nobody knows—and nobody is able to make a convincing prediction. This example serves to highlight our present level of the understanding of pore formation and to emphasize the viewpoint of the authors: pore formation in Si and all the other phenomena listed above (especially oscillations) are closely related.

This is a departure from more conventional approaches that try to model pore formation independently of all the other phenomena. We will therefore include the present status of a general model of the electrochemistry of Si in a final section and apply it to pore formation in Si.

Making porous Si in one of its many manifestations demands specific sets of parameters and some control of the etching process. While some pore morphologies are unique expressions of special parameters, others can be obtained for many, sometimes widely different conditions. With applications in mind, which set of parameters is best suited to the task—including economic considerations? While there are no simple answers at present, some guidelines can be given. The second section therefore attempts to correlate the zoology of macropores in Si and the most important ingredients from the available parameter space.

The third section deals with applications of macropores, the fourth and fifth with mesopores and micropores, respectively. While we try to review all potential applications presently pursued in the scientific/engineering communities together with specific problems, open questions, and emerging applications, it goes without saying that there are certainly some activities in the laboratories that the authors are not aware of—either because we failed to notice them or because they are (totally or partially) kept confidential on purpose. To compensate for this, there are some unpublished results that the authors are aware of and that will be included. In total, we cannot claim completeness in the listing of the application oriented work in this field and not always substantiate certain statements by citations.

1.2. Pores, electrolytes, and nomenclature

There is a large and growing diversity of pores in Si. Typical dimensions from 1 nm to 10 μm and morphologies from sponge-like to perfect-cylindrical are encountered. In what follows we will first define some terms useful for discussing the geometry and morphology as well as the production and application of pores. First, we will distinguish the three major types of electrolytes in use today.

- Electrolytes derived from the HF–H_2O system; called ''*aqueous electrolytes*'' and abbreviated with ''aqu''. This includes not only all mixtures of HF (commonly 49% p.w.) with water, but also fluorine bearing salts dissolved in H_2O (e.g. NH_4F), additions of ethanol (C_2H_4OH) and/or acetic
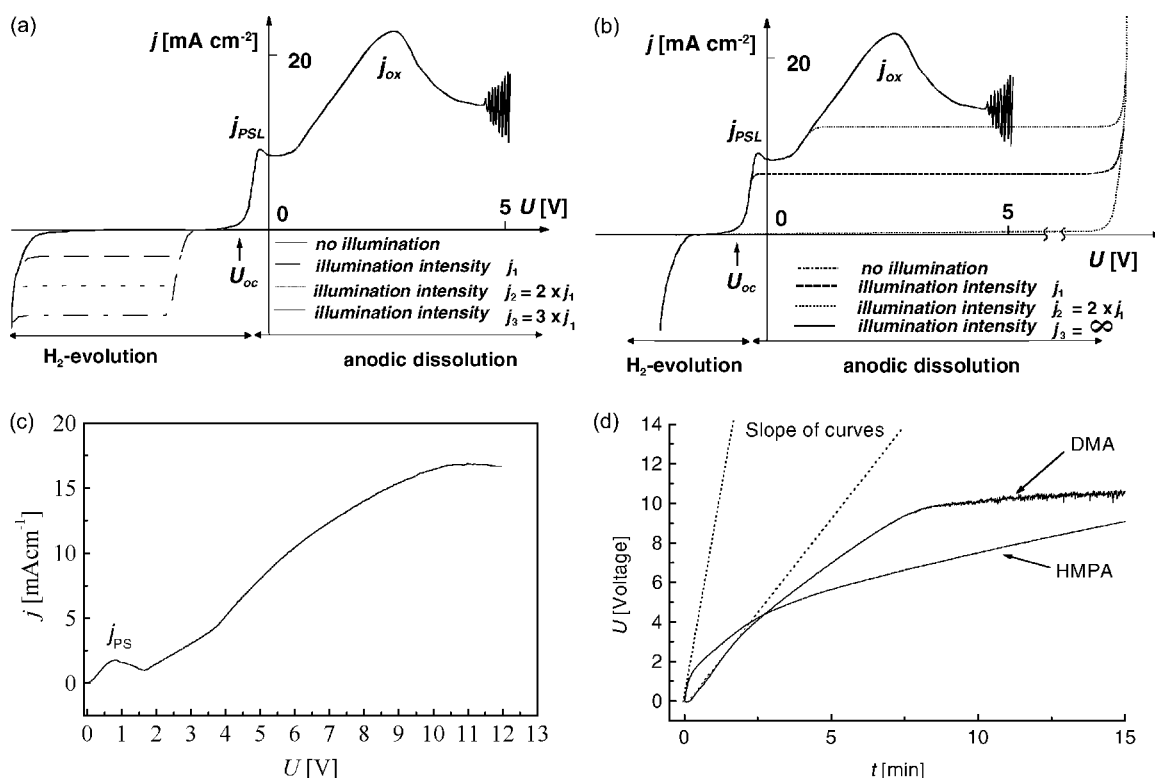
Fig. 1. Representative $I(V)$ characteristics: (a) aqu electrolyte, p-type Si; (b) aqu electrolyte, n-type Si; (c) org electrolyte (FA); (d) $U(t)$ for ox electrolytes. The PSL-peak is indicated by j_{PSL}.

acid (C_2HOH), or anything else that serves to reduce surface tension, adjusts the pH-value or the viscosity, or simply helps to get the desired results for unknown reasons. The nominal concentration of F (in any form) may range from 0.001 to 49%. All aqueous electrolytes have in common that a "PSL-peak" (see Fig. 1) is found in the $I(V)$-characteristics and that they are rather strongly oxidizing, i.e. tend to form SiO_2.

- Electrolytes mixing HF and an organic solvent (always including some water coming from adding HF (49%)). This class will be called "*organic electrolytes*" ("org" for short). There is a large number of organic solvents that have been used; most prominent, perhaps, is acetonitrile (MeCN), dimethylformamide (DMF), and dimethylsulfoxide (DMSO). While there might be some confusion with HF/ethanol mixtures which we count among the aqu electrolytes as explained above, the meaning is sufficiently clear in practice. Organic electrolytes so far have in common that their $I(V)$-characteristics do not show a PSL-peak. While it is possible that the PSL-peak is actually there but hidden due to the usually large resistance of the org electrolytes (which means that the series resistance of the system dominates the characteristics), it will be reasoned in Section 2 that this is a decisive feature of most (not necessarily all) org electrolytes and intimately linked to their "oxidizing power" (see later), which can be rather small. In any case, the absence of a PSL-peak gives a clear signal that formation models intimately tied to the current density j_{PSL} at the PSL-peak are limited in their application range.
- Electrolytes for anodic oxidation (called *oxidizing electrolytes*; abbreviated "ox"); always without F^- ions and containing some oxidizing reagent. Most common electrolytes without a HF addition fall into this category and we may classify their "oxidizing power" according to how well they

form an oxide on Si. In practical terms, this is easily measured by performing a constant current experiment. Due to the oxide being formed (but not dissolved), the voltage has to rise in order to keep the current constant. In the beginning of such an experiment, the $V(t)$-curves are always linear and the value of the slope dV/dt will be used as a measure of the "oxidizing power" of the oxidizing electrolytes, Fig. 1d shows some typical characteristics. "Oxidizing power" in the context of this paper is thus a well defined entity and will now be used without quotation marks in the remainder of the paper. Pure ox electrolytes have only limited applications, but may provide a key for the understanding of the electrochemistry of Si.

There is one more (potentially large group) of electrolytes not covered in this scheme which one might call "mixed electrolytes". This set contains everything not contained in the sets defined above, but so far not much practical significance has emerged. Examples that can be found in the literature include H_3PO_4 (by itself an "ox" electrolyte) with a dash of HF [32], absolutely water free org electrolytes [33], or diluted HF with some CrO_4 [34]. As the need arises, we will pinpoint these cases by mixing the symbols; the latter electrolyte than is designated (aqu + ox).

Next, we define some nomenclature regarding pores. According to the IUPAC standard, we must distinguish three categories by looking only at the parameters (average) pore diameter and (average) distance between pores, i.e. at the *geometry* of the pores.

- *Micropores*, with pore diameters and pore distances (from now on subsumed under "geometries") <10 nm.
- *Mesopores*, with geometries in the 10–50 nm region.
- *Macropores* with geometries in the >50 nm region.

Note that the *geometry* of pores does not contain much information about their *morphology*. This term will be used as the collective identifier for properties like the shape (smooth, branched, facetted, ...), orientation, or interaction of pores, that are independent of the geometry.

All three kinds of pores can be obtained under a variety of (sometimes very different) conditions, and with widely differing morphologies. Key parameters are the electrolyte type (aqu, org, ox), the HF concentration, the doping type and level of the Si (n, n^+, p, p^+), and in some cases the illumination state (back side illumination (bsi), or front side illumination (fsi)). We will use these abbreviations to extend the classification of pores in a self-explaining notation: n-macropores(aqu/bsi) or n-macropores(aqu/fsi) thus are macropores produced in n-Si under backside or frontside illumination using aqueous electrolyte; p-macropores(aqu) or p-macropores(org) denote macropores obtained without illumination in p-type Si with aqueous or organic electrolytes; and n^+-macropores(aqu + ox) denotes macropores obtained in heavily doped n-type Si in a mixture of an aqueous electrolyte with the addition of an oxidizing electrolyte, respectively.

It is absolutely essential to adhere to this nomenclature to avoid considerable confusion—the examples chosen demonstrate this point: macropores can be obtained under a variety of very different conditions; Fig. 2 illustrates this. This was a rather unforeseen development since the discovery of smooth cylindrical ("perfect") n-macropores(aqu/bsi) with large aspect ratios by Lehmann and Föll in 1990 [35]. While this kind of macropores was investigated in some detail, only few investigations dealt with the rest.

The basic IUPAC distinction of pores into micro-, meso-, and macropores is far to coarse and not particularly well suited to unambiguously sort out pores in Si. The term "macropore" usually is associated with smooth cylindrical pores in the 1 μm region, and no such macropores have been observed (so far) in the 50 to 500 nm region to which the term nominally applies. Contrariwise, while n^+-, p^+-mesopores(aqu) are indeed (mostly) found within their admissible size range of 10–50 nm, it is simply not useful to call pores "macropores" that have a morphology exactly like
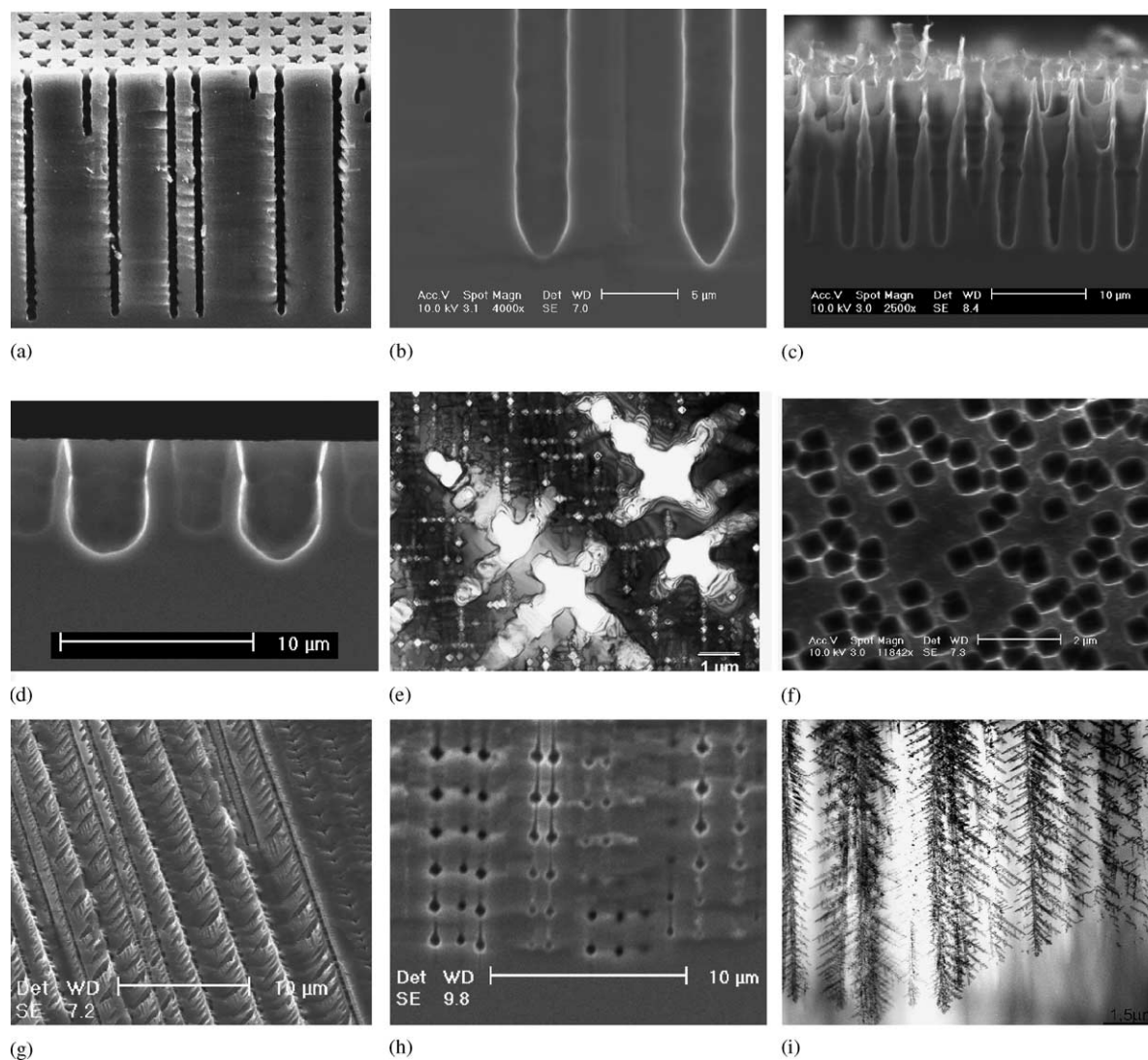
Fig. 2. Some examples demonstrating the variety of pores found in Si: (a) seeded n-macropores(aqu/bsi) from the first experiments performed [35], (b) random n-macropores(aqu/bsi) from [39], (c) n-macropores(aqu/fsi), (d) p-macropores(aqu), (e) n-macropores(org/bsi) as seen in pore growth direction by TEM, (f) n^+-macropores(aqu + ox), (g) n-macropores(org/bsi), (h) n-macropores(org/bsi) with sin modulated current and non-linear response, (i) n-macropores(org/bsi).

"proper" mesopores as soon as their diameter exceeds 50 nm. "Break through" pores, e.g. obtained in n-type Si in the dark at large potentials (and in all electrolytes), while very similar in appearance to n^+-mesopores(aqu), tend to be a bit larger in diameter and may exceed the 50 nm limit, but still will be called n-mesopores(dark) in this paper.

It should be noted that current research produced "pores" that cannot be adequately described in this system. Examples are the two-dimensional "trenches" and "wings" [22] observed under conditions that also produce p-macropores(org) and n-macropores(org/bsi), respectively, cf. Figs. 6b and 15b.

Why do pores form under a wide range of experimental conditions and what determines their geometry and morphology? As stated before, the authors are of the opinion that pore formation

cannot be understood by itself, but must be seen in a larger context that includes the other salient features of the Si electrode. A first attempt at such a generalized model, including pore formation, has been proposed by the authors [10,12,20]; it attempts to describe all features of Si electrochemistry as the expression of the interaction between stochastically occurring "current bursts" (CB) which are localized in space and time. This model is called the current burst model (CBM) and will be briefly described in Section 7.

1.3. Pore formation models

It is not necessary to go into details of the various pore formation models in order to obtain some basic understanding of what determines pore parameters. No matter what kind of pores results from some experiment, they always have some characteristic dimensions—average diameter, average distance, spacing between branches—and all these length scales are usually rather well defined. While not many quantitative investigations on characteristic dimensions have been made, it is safe to say that pore formation of any kind (almost) always defines a specific length scale prevalent in the Si—electrolyte system employed that expresses itself in the (average) pore geometry and morphology. Any model thus must ultimately give a reason for the actual scale found in the pores under investigation in order to explain the geometry. Note, however, that the presence of a specific length scale does not necessarily explain pore formation per se.

The most advanced models for pore formation essentially give a reason for pore nucleation and stability and define a characteristic length scale. The most important length scales proposed are as follows.

- *Width of the space charge region* (L_{SCR}). This was first proposed by Lehmann and Föll [35] not only as the major parameter governing pore geometry and morphology, but also as the only cause for the actual formation of n-macropores(aqu/bsi). The model has been quantified to some extent [36] and has been used with great success to produce beautiful pore structures for many applications [37,38]. However, while L_{SCR} and other effects due to the space charge region undoubtedly are very important for pore parameters, it has become obvious that L_{SCR} is not sufficient to explain macropores in general [39], not least because it relies heavily on the presence of a PSL-peak which is not observed for most org electrolytes.
- *Pore tip radius* L_{AV} inducing avalanche break down. At high field strengths at pore tips with a sufficiently small radius, avalanche break down necessarily occurs, supplying plenty of carriers to drive the electrochemical reactions—a process often exploited in n-type semiconductors where holes are scarce. While not a new idea [40], Lehmann et al. give a fully quantitative treatment and apply this effect to pore formation in general [41]. However, while avalanche break down will occur under certain conditions, it will be a locally and temporarily self-stopping process if some oxide formation occurs because this will locally decrease the field strength. Seen in this context, L_{AV} will give the smallest dimensions possible for pores obtainable under conditions where it occurs. Smaller pores will simply grow to a diameter just above L_{AV} and avalanche break down only happens "every once in a while and here or there"—stochastically, in other words. In addition, the relative avoidance of avalanche break down will lead to round pore tips having a constant field strength at any point.
- *Diffusion instabilities*, well known from the growth of dendritic crystals (e.g. snowflakes) may induce gradients in the hole concentration with a typical dimension L_{DIF} and thus induce or stabilize pores with that dimension. This case was treated in detail by Chazalviel et al. [42], Smith and Collinsbut [43] since L_{DIF} is always tied to the diffusion length or Debye length of the holes,

L_{DIF} is too restricted to account for all effects. It appears, however, that L_{DIF} is an important length scale for some p-macropore (org) systems.

- *Quantum wire effects* at length scales below $L_{QU} \approx 1$ nm that prevent the movement of holes to the Si–electrolyte interface. This effect was invoked to explain the formation of micropores [44]. However, while L_{QU} may define the minimum distance between micropores, it has nothing to say about the diameter of the micropores itself.
- Another typical length, often overlooked, is the *spacing between lithographically defined nuclei*, L_{NU}, which is totally independent of the system parameters and thus a truly extrinsic length scale.
- The CBM finally defines a typical length scale, too, called the *correlation length L_{CO}* of the interaction between localized current bursts [12,20]; see Section 7 for details.

All these length scales definitely exist—at least in a subset of the available parameter space—and influence the geometry and morphology of pores. It is, however, not always clear which scales dominate the pore formation process and what will happen when major conflicts of length scales are unavoidable. For example, a clear conflict of scale occurs when the extrinsic length scale L_{NU} is too different from L_{SC}—it is simply not possible to obtain macropores spaced at distances much larger or much smaller than L_{SC}. Another conflict of scales occurs if one tries to produce macropores with diameters much smaller than L_{AV} or L_{CO}—and this is as much a prediction as a (largely unpublished) experimental fact.

It should be realized that there is a large body of experimental results that was never published, especially if the experiments were made with a particular goal in mind that could not be achieved. Etching well-formed macropores in the sub-μm region, e.g. has been tried in several laboratories; but only one success was reported for a 0.5 μm geometry after extensive work (including growing a special Si crystal) [45] while the unsuccessful attempts at even smaller spacings have not been published (including the efforts of the authors). Defined modulations of macropore diameters fall in this category, too.

2. Formation of macropores

2.1. Macropores in n-silicon obtained in aqueous electrolytes with back side illumination

Since n-macropores(aqu/bsi) are the best known species of macropores, we will consider them in some detail before treating the other kinds. "Perfect" pores with very large aspect ratios have been obtained for this species, and "perfect" means not only smooth pore walls, but also smooth cross-sections (albeit not necessarily circular) and constant diameter with depth.

The n-macropores(aqu/bsi) were first predicted by one of the authors and then found in a suitably designed experiment [35]. The prediction was based on results obtained in general electrochemical experiments with Si which produced precursors of n-macropores(aqu/fsi), cf. Fig. 13a). The basic idea was that the system n-Si/electrolyte is reversely biased in electrical terms, and that any bending of the prominent space charge region (SCR) in the Si by proto-pores would focus some of the holes produced by light on the pore tip. If holes would be available from the back side only, e.g. by back side illumination of samples with sufficiently large diffusion lengths for the minority carriers, they would be focussed by the SCR on the pore tips and macropores should grow with constant diameters to considerable depths.

Experiments were performed with lithographically defined nucleation (simply by using typical DRAM trench masks) and proved immediately successful, giving some weight to the simple "space

charge region pore formation model'' (SCR-model) invoked. Further investigations and optimizations, mostly by Lehmann and coworkers (e.g. [36,38]), supplied some theoretical background and developed this etching technology to a fine art.

In particular, Lehmann proposed a simple formula (''Lehmann's formula'') that related the cross-sectional area $A_{po} \approx d^2$ ($d =$ diameter of the pore) of the pore to the area $A_{cell} = a^2$ ($a =$ lattice constant) of a unit cell of the pore lattice and to the current density j via

$$\frac{A_{cell}}{A_{po}} = \left(\frac{d}{a}\right)^2 = \frac{j}{j_{PSL}} \tag{2.1}$$

with $j_{PSL} =$ current density of the PSL-peak of the system (cf. Fig. 1). For ''random'' pores obtained without predefined nucleation, or non cubic pore lattices, averages of d and a have to be taken. Since the PSL-peak depends almost exclusively on the HF concentration and is thus a known quantity, Lehmann's formula is of considerable practical value.

The reasoning behind the formula is easy to understand: if stable macropores form and grow, all current must flow through the macropores and the current density in a pore is then

$$j_{pore} = \frac{jA_{cell}}{A_{po}}. \tag{2.2}$$

The pore thus has a ''choice'' of adjusting itself to an optimum current density by adjusting its diameter, and j_{PSL} is a logical choice, being the only special current density in the characteristics which, moreover, signifies the switch-over to electropolishing.

Obviously, Lehmann's formula is only applicable to n-macropores(aqu/bsi) under conditions where the applied potential is significantly larger than U_{PSL}, the potential corresponding to the $j_{PSL\text{-}peak}$, and perhaps to some extent to n-macropores(fsi), but not to p-macropores(aqu), and especially not to p, n-macropores(org), because the relevant $I(V)$-characteristics do not contain a PSL-peak.

Eq. (2.1) would allow any pitch d/a, i.e. arbitrarily large or small pores at any spacing. This is not realistic, however, because the basic premises of the SCR-model was that the space charge region must be bend around a pore but not penetrate between the pores. This imposes somewhat fuzzy limits on d and a: it must be expected that stable pore growth is only possible if d and a are in the same order of magnitude as L_{SCR}, the width of the space charge region. This is illustrated in Fig. 3.

The validity of Lehmann's formula is demonstrated in a series of experiments where the distance a between pores was varied between 4 and 64 μm while the pitch d/a was kept constant; some results are shown in Fig. 4.

It can be seen that if a is too small, some pores stop to grow, and if a is too large, the pore surfaces become rough and that the diameters are smaller than expected. While Grüning et al. showed that there is still preferred carrier flow to the pore tips even for spacings larger than 2 L_{SCR} [46], there is, however, still stable pore growth at distances where carriers can easily penetrate the area between the pores (corresponding to Fig. 3b) which gives a definite indication that something else besides the diversion of carriers to pore tips by the SCR must stabilize pore walls against further dissolution. Contrariwise, it is not clear from the SCR-model alone, why case (d) in Fig. 3—making very thin pores at a relatively large spacing—is apparently not possible.

It is thus not easily possible to produce n-macropore(aqu/bsi) arrays with $d \gg 1$ μm, or $a \gg 5$ μm with standard Si samples. Noteworthy exceptions are the photonic crystals produced with n-macropore(aqu/bsi) arrays at dimensions of 0.5 μm [45] using a specially grown Si crystal (FZ, highly doped but still with a large diffusion length of minority carriers), and, at the other extreme, pore arrays with >100 μm dimensions [47].
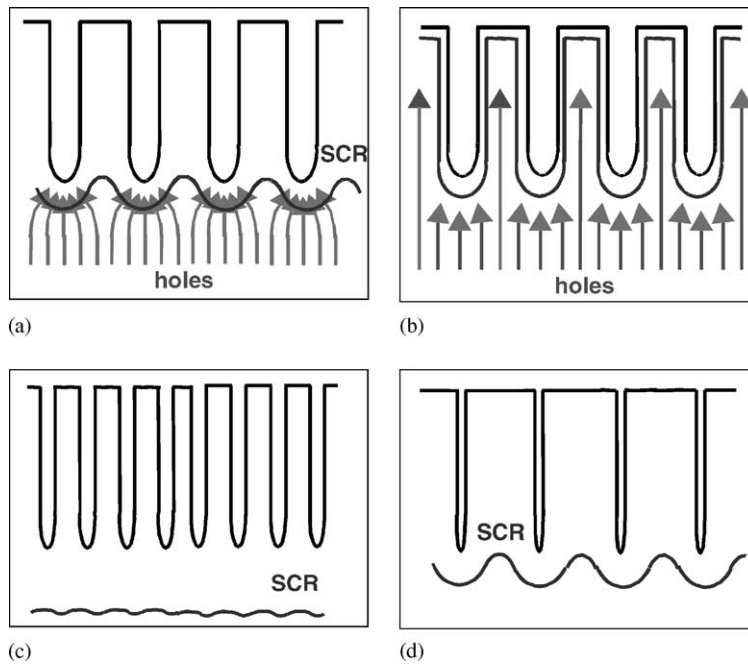
Fig. 3. Four basic cases of SCR controlled n-macropore(aqu/bsi) growth: (a) space charge region width L_{SCR} matched to d and a; (b) $a \gg L_{SCR}$; (c) $a \ll L_{SCR}$; (d) $a \approx L_{SCR}$, $d \ll L_{SCR}$.

From these considerations a few more inferences can be made with respect to achievable pore geometries.

- Without extrinsically defined pore nucleation, "random" pores will result and their average diameter $\langle d \rangle$ and spacing $\langle a \rangle$ can be expected to be comparable to L_{SCR}. One study of this topic
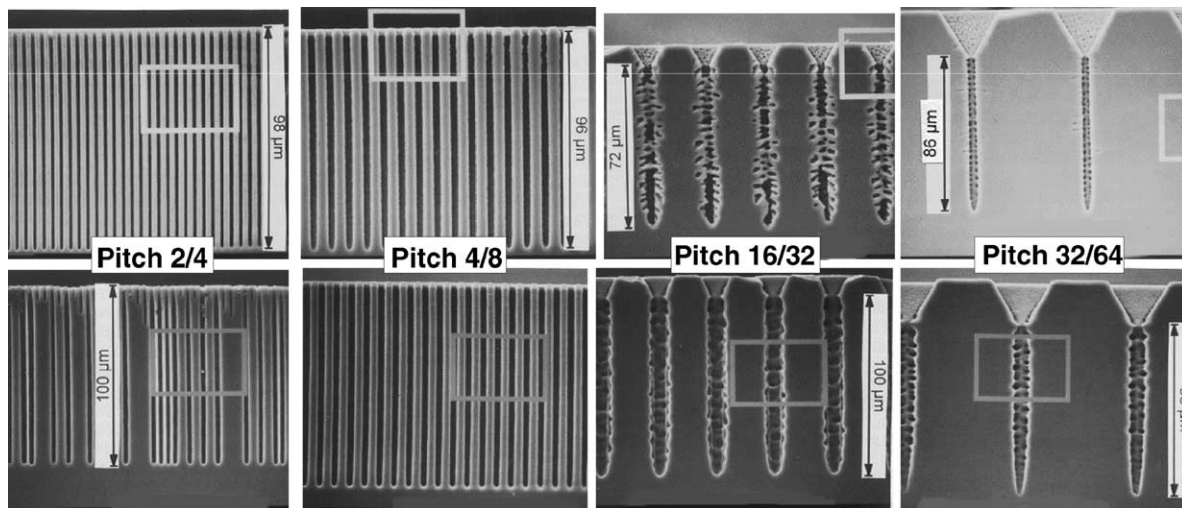
Fig. 4. The n-macropores(bsi) etched in 4% HF solution at 2 V with pre-structured nuclei at variable distances from 4 to 64 μm and etching currents and times adjusted to yield constant pitch and depth. Upper row: 5 Ω cm ($L_{SCR} \approx 1$ μm), lower row 40 Ω cm ($L_{SCR} \approx 3$ μm) Si samples.

has been made [39] and while the general prediction is correct, there are clear exceptions for highly doped Si.

- Etching n-macropores(aqu/bsi) in defined areas only, with the help of, e.g. a Si_3N_4 mask, has been tried repeatedly, but unsuccessfully. While macropore arrays with good quality could be obtained in the interior of the unmasked area, there will always be some macropore growth under the mask—in rather irregular fashion. This indicates that whatever mechanism protects the pore walls from etch attack under conditions as, e.g. shown in Fig. 4 for large lattice constants a, is not sufficiently strong under the pertaining conditions to keep the walls totally inert. While it is too early to say that this task (which is of obvious technical importance) can never be achieved, it is probably safe to say that the pore etching and pore wall passivation mechanisms must be much better understood for a successful solution of this practical problem.

- Intentionally introduced defects in regular arrays (e.g. missing pores) are possible, as long as the distances between the remaining pores do not become too large. The pores next to the defects will then increase their diameter slightly to accommodate the surplus holes. It is not possible, however, to produce isolated pores because the many holes not flowing to the pore tip will eventually either induce random nucleation of pores, or erode the pore walls of single pores, or both.

- The pore diameter cannot be adjusted for individual pores, but only for the pore assembly by varying the etching current during etching. As long as the chemical processes are fast enough, the diameter as a function of depth z should follow the current modulations in time, or $d(z) = vj(t)$ with $v =$ growth velocity of the pores. Inducing controlled diameter modulations, however, has proved to be surprisingly difficult. While it is possible in principal [48], it is often observed that $d(z)$ does not follow $j(z)$ but reacts rather non-linearly to current modulations as illustrated in Fig. 2h.

- While Lehmann's formula should apply to all HF concentrations (which essentially define j_{PSL}), the general experience is that it is very difficult if not impossible to obtain smooth n-macropores(aqu/bsi) for HF concentrations above about 10%. This severely limits the growth rate v for n-macropores(aqu/bsi) to (rule of thumb) ≈1 μm/min.

- For very smooth pores and large aspect ratios, all etching parameters have to be "just right". This includes the HF concentration, the voltage, the temperature, and the flow of the electrolyte. Changing one parameter without properly readjusting the others will tend to result in less perfect pores.

- For deep pores, diffusion effects have to be taken into account. The diffusion of molecules into and out of the pores becomes more difficult as the pore depth increases, while the diffusion of holes to the pore tip becomes easier as the distance between the pore tip and the illuminated backside decreases. Both effects change j and j_{PSL}, so simply keeping $j =$ constant during an etching experiment will not necessarily keep the pore diameters constant. Lehmann analyzed these effects in detail [36] and developed a software that compensates for the chemical diffusion effects during etching taking into account also the temperature dependence of the processes. Several groups active in the field use this software and thus automatically obtain the geometric parameters independent of temperature and diffusion—in principle. There are, however, still pronounced effects, particularly with respect to the etching temperature (cf. [9]), that are not included in the software (or not even understood).

- It may be useful in certain instances, to over-etch the n-macropores(aqu/bsi) by a (usually very gentle) purely chemical etch. This will enlarge the pore diameters and smooth the walls if done right.

One more interesting point concerning n-macropores(aqu/bsi) is the dependence of the pore morphology on the sample orientation. Most models are silent on this point (they would be fully applicable to amorphous semiconductors, too); the expectation at best would be that pores grow
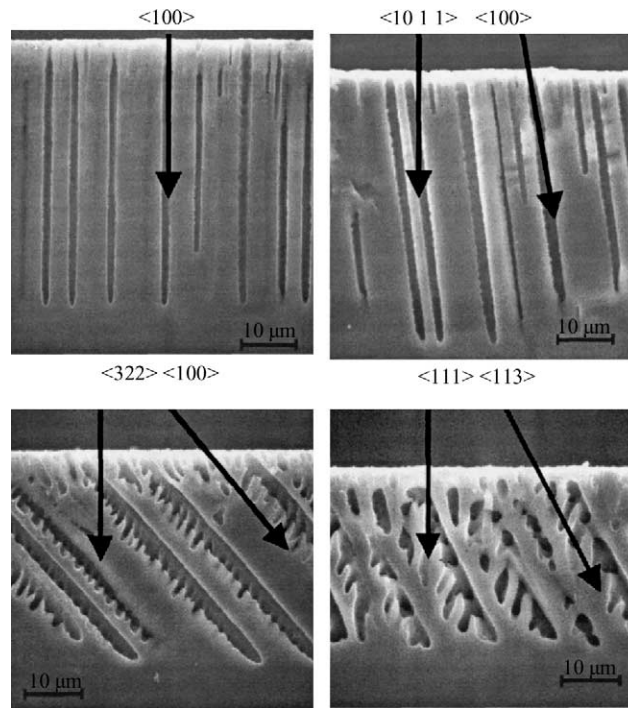
Fig. 5. Orientation dependence of (random) n-macropores(aqu/bsi). The substrate orientation is (a) $\langle 1\,0\,0\rangle$, (b) $\langle 10, 1, 1\rangle$, (c) $\langle 3\,2\,2\rangle$, and (d) $\langle 1\,1\,1\rangle$. In (d) $\langle 1\,1\,3\rangle$ oriented pore tripods result.

directly towards the source of the holes, i.e. perpendicular to any surface. This is decidedly not the case. Detailed investigations [21] showed that n-macropores(aqu/bsi) grow exclusively in $\langle 1\,0\,0\rangle$ directions and (occasionally, if all available $\langle 1\,0\,0\rangle$ directions are steeply inclined) in $\langle 1\,1\,3\rangle$ directions. Their morphology is always describable as a main pore in one of this two directions and side pores or branches in some of the others. Fig. 5 shows some examples. This fact, again, demonstrates drastically that the SCR-model alone cannot account for all n-macropore(aqu/bsi) features.

The dependence of the pore morphology on sample orientation is just as complex for other kinds of pores, too; it will be covered in the appropriate sections. Whereas not many practical uses for the peculiarities of orientation dependence have been envisioned so far (for an exception, see Section 3), some more ideas are emerging. In any case, orientation dependence of pore growth is a major issue for modeling purposes and thus may be beneficial for applications in an indirect way.

In total, producing arrays of "perfect" n-macropores(aqu/bsi) with defined dimensions and possibly including defects (e.g. for photonic crystals), while easy in principle, requires carefully designed experiments with plenty of fine tuning, even on the laboratory scale (with typical sample dimensions of a few cm^2). Etching n-macropores(aqu/bsi) in standard Si wafers of at least 100 mm, possibly 300 mm diameter, requires a major investment (in time and money) into the construction of a suitable apparatus. So far, few groups have attempted this, but it can be done as shown by Lehmann and Grüning [38] and van den Meerakker et al. [49]. We will come back to this point in Section 6.

2.2. Other types of macropores and related structures

The n-macropores(aqu/bsi) have been targeted for a number of applications and several projects are under way towards a commercial product; this will be covered in Section 3. This is not (yet) the

Table 1
Comprehensive listing of macropore types and two-dimensional structures observed so far

Type	Remarks
n-Macropores(aqu/bsi)	Oldest and ''best'' types of macropores, ''Lehmanns formula'' applies, SCR limits distances; diameter limitation uncertain but diameters <0.8 µm difficult to obtain. Maximum depth >600 µm achieved. Obtained for $j < j_{PSL}$; but no ''good'' pores for [HF] > 10%; $U > 5$ V. Temperature is important
n-Macropores(aqu/fsi)	Not much investigated
n-Macropores(org/bsi)	Only investigated for DMF/4% HF. ''Strange'' morphologies, mix with mesopores, peculiar growth dynamics
p-Macropores(aqu)	Observed for ''low'' currents and HF concentrations (otherwise micropores result), potentially useful because relatively easy to make
p^+-Macropores(aqu + ox)	Only known exception to the rule that only mesopores form in highly doped Si. Potentially useful for small diameters
p-Macropores(org)	Large range of macropores observed, from shallow depressions to macropores rivaling the best n-macropores(bsi). Decisive parameters are electrolyte conductivity, ''oxidizing power'', ''passivation power'' and dielectric constant. Large potential for applications because SCR restrictions are less severe
Secondary macropores	Long nucleation phase, always filled with mesopores
p-Trenches(org/masked)	Two-dimensional trenches instead of macropores may result if a Si_3N_4 mask is used to define areas to be etched
n-Wings(org/bsi)	Two-dimensional cavities bound by {1 1 1} planes on the upper side may occur, with n-macropores(org/bsi) hanging down like stalagmites

case for the other types of macropores—they are too new for that. However, n-macropore(aqu/bsi) technology is not only rather difficult (requiring backside illumination) but has several limitations that the other macropore types may or may not have. We will therefore cover these new developments in some detail, too.

As already mentioned, macropores now can be made in a variety of very different ways, Table 1 gives a short overview together with the more outstanding features.

Some entries, suggested by symmetry, are missing. Only first experiments on n-macropores(org/fsi) exist (cf. Fig. 13), while n^+-macropores(aqu + ox) seem not to exist; a search for them has been made but was not successful—mesopores were obtained under all conditions tried [34].

The entry ''secondary macropores'' needs an explanation. This kind of macropores forms if mesopores (or possibly micropores) are formed as the primary pores (responding to a small primary length scale of the system) while a large secondary length scale eventually causes an instability of the pore front. Bulgy secondary macropores filled with mesopores may result, e.g. because of diffusion instabilities; cf. Fig. 7f).

Besides (macro)pores—always defining an one-dimensional structure with a length in *z*-direction (potentially) much larger than its lateral *x*- and *y*-dimensions—two-dimensional structures have been observed recently that occur in close connection with macropores [50]. The first of these new etching features is obtained if p-macropore(org) etching is tried in defined areas only, the rest being protected by a Si_3N_4 mask (without a buffer oxide as commonly used in microelectronics). Depending on the etching conditions and in particular on the nitride thickness, a trench (or fissure) along the mask edge is observed that penetrates much deeper into the Si than the p-macropores(org) in the inside of the open area. Fig. 6 gives an example, for details see [50]. In what follows we use the name *trench* for this structure which should not be confused with the ''trenches'' in integrated circuits (DRAMs; the microelectronic community calls holes or pores ''trenches'' (as in ''trench'' capacitor) for rather obscure reasons) or with the ''trenches'' to which some older pore literature referred on occasion (e.g. the first n-macropore(aqu/bsi) paper [35]), when pores were meant. Trenches have obvious potential uses; this will be discussed later.
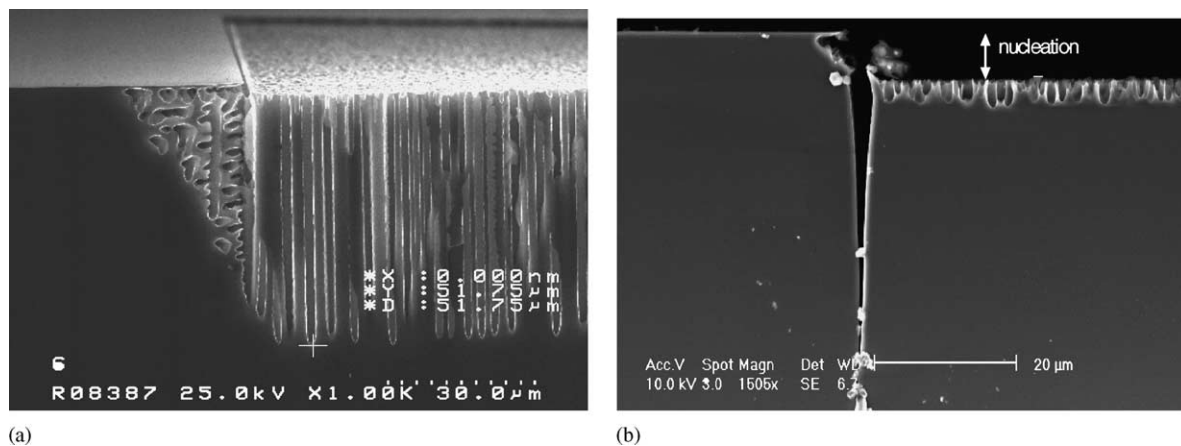
Fig. 6. (a) Regular p-macropores(org/DMF), showing under-etching of the nitride mask. (b) A ''trench'' running along the mask etch together with shallow p-macropores(org/DMF) obtained under similar conditions.

A second two-dimensional etching structure (''wings'' [51]) was found in connection with n-macropores(org/bsi) and will be treated there.

2.3. Macropores in p-silicon obtained in organic electrolytes

The first p-macropores(org) were found by Propst and Kohl in 1994 [33]. In the following years, many papers have been published dealing with new kinds of p-macropores(org) obtained by using different kinds of organic electrolytes, e.g. [52–56]. While it first appeared that p-macropores(org) were limited to Si with a rather high resistivity of $\geq 100\,\Omega$ cm (resulting in relatively short and ''bulgy'' pores), Ponomarev and Levy-Clement [53] were the first to etch macropores on $1\,\Omega$ cm (1 0 0) and (1 1 1) orientated Si substrates using different organic electrolytes. Christophersen et al. finally found very stable growth conditions for p-type macropores (org) allowing for pore depths up to 400 µm [54]. Fig. 7 gives a sample of the kinds of p-macropores(org) that could be obtained so far.

This situation was (and is) somewhat puzzling, because the SCR-model generally used to explain n-macropore(aqu) formation did not seem to allow for macropore formation in p-type Si at all. The avoidance of holes between the pore walls with the bsi—''trick'' is not possible, the space charge region can never be very wide, and thus should have much less ''focussing'' power.

The p-macropores(org) may be coming close to applications. Ohji et al. were able to build free standing silicon structures based on electrochemically etched p-macropores(org) using pre-structured p-type silicon [55], while Chao et al. presented deep p-macropores(org) with depths up to 400 µm and found that pre-structuring significantly stabilized pore growth [56]. Possible advantages in comparison with n-macropores(aqu) are a somewhat simpler cell design (no backside illumination necessary) and (so far) unknown limitations—maybe etching speeds could be higher, or pores with a smaller pitch are possible? On the other hand, the electrolytes are often very aggressive (only polyfluorated materials might be usable for the electrochemical cell) and expensive to get rid of in an orderly fashion.

We may consider two deep questions in connection with p-macropores(org)—one more fundamental, one more practical.

1. What are the mechanisms responsible for formation of p-macropores(org) and which parameters determine geometry and morphology?
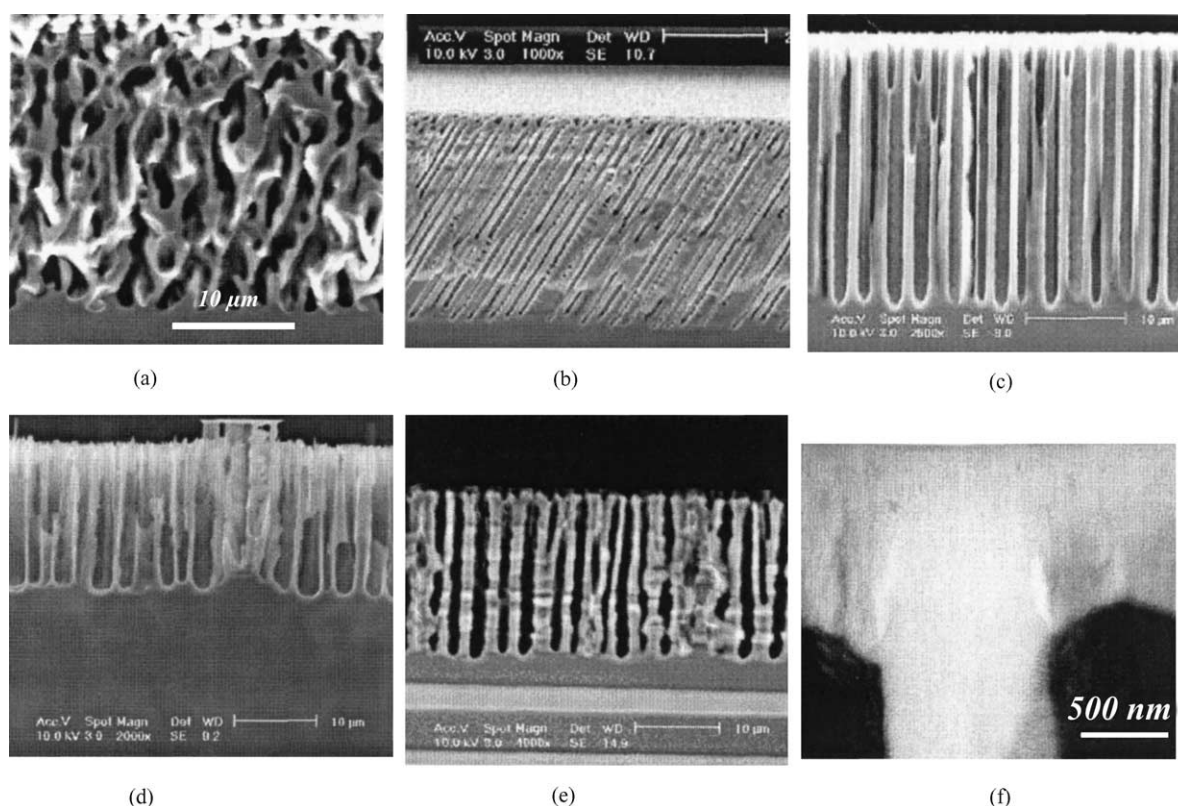
Fig. 7. Some samples of p-macropores(org) with 4 wt.% HF: (a) MeCN, {1 1 1} sample; (b) DMF on {5 1 1} Si; (c) DMF—perfect pores; (d) HMPA; low current density—bulgy pores; (e) MeCN + diethyleneglycol (protic additive); (f) TEM of secondary pore formation on {1 0 0}.
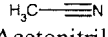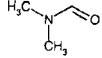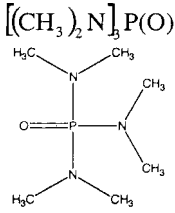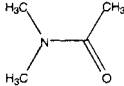
2. Given the inexhaustible (chemical) parameter space, how do we find optimized etching conditions for a particular task, i.e. electrolyte composition, current density, voltage, and temperature?

Exhaustive answers to these questions are not yet in. We will try to give partial answers by listing some generalized points extracted from a host of experiments with p-macro-pores(org), and by some speculations based on the CBM. First, however, the major organic compounds used so far are listed with some of their properties in Table 2. The numbers in the entry "oxidizing power" give the slope of the $U(t)$ curves obtained for anodic oxide formation with a constant current density as discussed before.

The HF addition is always 4% HF by weight if not otherwise stated. Since the HF is usually taken from a standard 49% HF solution, organic electrolytes therefore will always contain some water coming from the HF. Exceptions are the studies reported in [33] where essentially no direct macropores were found but, as far as indicated, only "second order" macropores according to our nomenclature (and expectation).

So far, there are no clear and simple rules for the pore geometry comparable to "Lehmann's formula" for n-macropores(org). At present, the work of Chazalviel et al. [42], considering mostly diffusion instabilities, may come closest to making some predictions, especially for the case of low doped (and amorphous) Si. A few general points are as follows.

Table 2
Organic electrolytes used in Si electrochemistry and some of their major properties

Symbol	Formula name	Polarity (DK)	Oxidizing power
MeCN	H_3C—$\equiv$N Acetonitrile	6.2	Very weak; slope of anodic oxide, 0 a.u.
DMF	Dimethylformamide	6.4	Slightly oxidizing, 0.5 a.u.
FA	Formamide	7.3	Strong, 3.5 a.u.
DMSO	Dimethylsulfoxide	6.5	Mild oxidizing, 2.5 a.u.
HMPA	$[(CH_3)_2N]_3P(O)$ Hexamethylphosphoric triamide	6.6	Oxidizing, 6.5 a.u.
DMA	Dimethylacetamide	6.3	Mild oxidizing, 2.1 a.u.

- The doping of the Si is rather important. Increasing the doping level acts to some extend like increasing the applied potential. In general, high doping levels reduce the ability to form macropores [34,57]. Viewed relative to aqueous electrolytes, the switch-over to mesopores occurs already at lower doping levels.
- The p-macropores(org) tend to become more ''perfect'' if the oxidizing power of the electrolyte is not too small (at least 0.5 on our scale). Electrolytes with little oxidizing power as, e.g. MeCN, will hardly produce macropores at all, whereas electrolytes with strong oxidizing power (e.g. FA, comparable to H_2O or stronger) produce micropores instead of macropores.
- Stable growth to considerable depth also requires the availability of H or more precisely, it is related to the ''passivation power'' of the electrolyte in the context of the CB model. ''Passivation power'', like oxidizing power, is not a property of standard chemistry but has nonetheless a well defined meaning: it denotes the degree to which a given electrolyte can remove interface states in the band-gap of Si by covering a freshly etched surface with hydrogen. This is a measurable quantity in principle, but while preliminary measurements based on the ELYMAT technique [15] have been made, no reliable data exist at present. The following remarks are either based on circumstantial evidence or may be taken as predictions. It is therefore of importance whether the electrolyte is protic or aprotic (i.e. donates or accepts hydrogen) and, of course, the pH value may

be involved [58], but might not always be of prime importance [14]. In the CBM, H-passivation is the major process responsible for pore formation and it has been shown that additions of protic substances to an org-electrolyte change the pore growth in the expected way [22].

- The dielectric constant (DK) of the electrolyte must be considered. Essentially, the DK determines to which degree HF will be fully dissociated and thus "active". Electrolytes with a low DK tend to have a reduced HF "activity" which slows down the direct dissolution process and the oxide dissolution.
- The conductivity of the electrolyte is of course of considerable importance, too. It would be too naive to assume that the resistance of the electrolyte can be easily compensated for by increasing the voltage, because diffusion of species in the electrolyte can lead to phenomena similar to the diffusion of holes in the semiconductor and therefore introduce instabilities that cause, modify or interfere with pore formation, cf. [42,59].
- Temperature, circulation of the electrolyte, small additions of surfaces reactant, or bubbling with N_2 to remove oxygen dissolved from the air, may also be of importance.
- The nucleation of p-macropores(org) can be achieved by supplying pre-structured nuclei as in the case of n-macropores(bsi), but not many investigations have used this technique (see [36] for example). Homogeneous random nucleation, on the other hand, can be rather difficult and may only occur after a certain period of larger voltages intentionally supplied for the nucleation phase or automatically employed by the potentiostat if galvanic conditions are used, cf. Fig. 8.
- The orientation dependence of p-macropores(org) is similar to that of n-macropore(aqu), but often not quite as pronounced because the pores are often not well defined (cf. Fig. 7a).
- While the limitations with respect to pore geometries and morphologies are not known at present, recent experiments of the authors (following the guide lines from above and some rules derived from the CBM and published here for the first time) demonstrate that $(0.2\,\mu m \times 0.4\,\mu m)/0.2\,\mu m$ pitches are possible (Fig. 9)—a feat are often tried, but never achieved with n-macropores(bsi). The pores have rough walls, demonstrating the need of fine tuning any process that is to deliver "perfect" pores.

The listing above contains implicit claims with respect to certain electrolyte properties, derived from generalizations of measurements as shown in Fig. 10. More data concerning the correlation of p-macropores(org) and properties of the chemicals employed can be found in [22]. In essence, while these investigation stress the traditional chemical point of view and provide valuable data concerning the dependence of pore geometry and morphology on chemical properties and the conductivity of the
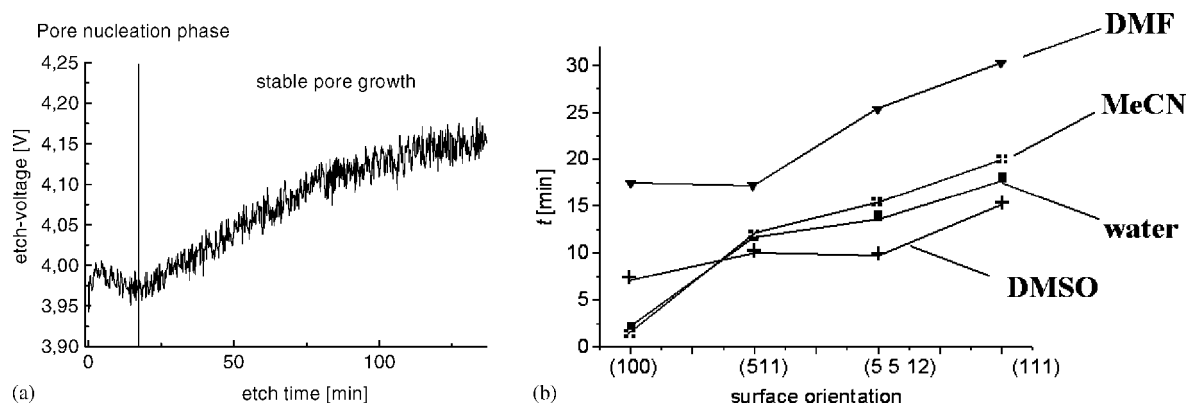

Fig. 8. (a) Development of the voltage over time for constant current and a DMF electrolyte. A nucleation phase, and a stable growth phase can always be identified. (b) Nucleation time for various electrolytes and surface orientations.
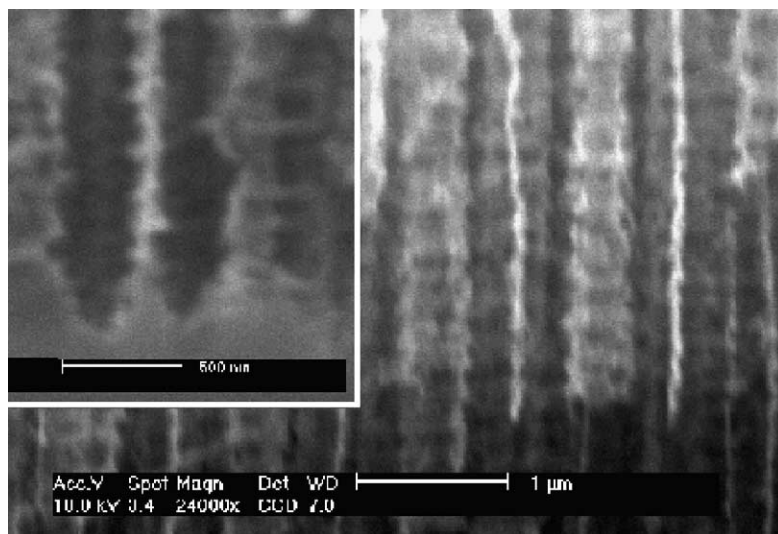
Fig. 9. First 200 nm macropores obtained by optimized organic electrolytes and etching conditions (the smallest pitch is perpendicular to the cleavage plane).
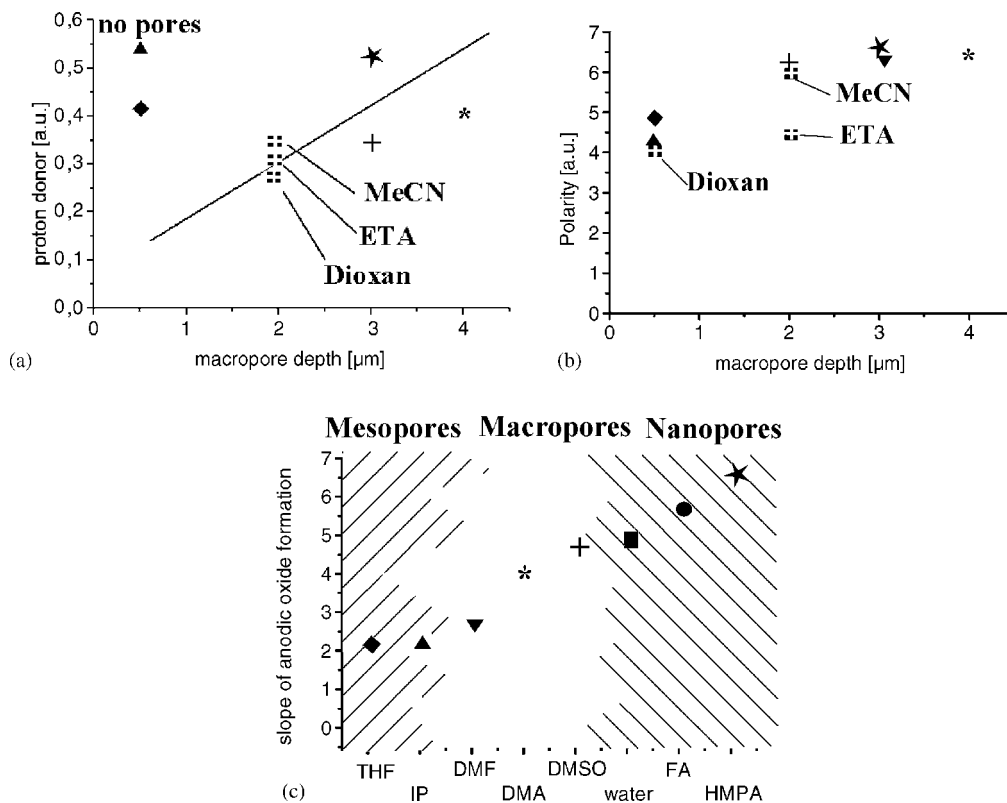

Fig. 10. Various correlations between p-macropore(org) properties and electrolyte properties. (a) Dependence of p-macropore(org) depth on the ability to donate protons of the electrolytes. The numbers are from [61]; the symbols were defined in Fig. 8b. (b) Polarity of organic electrolytes. It simply scales with the value of the dielectric constant or index of refraction. (c) Correlation of the oxidizing power and pore formation for various organic electrolytes (and H_2O for comparison).

Si, little information can be deduced with respect to the questions at the outset of this paragraphs from standard chemistry alone.

In this context, it is important to point out again formamide (FA), a new kind of org electrolyte with an oxidizing power exceeding that of water and used here for the first time. FA electrolytes do not produce p-macropores(org), but p-micropores(org) (cf. Fig. 26), exhibit a PSL-peak in the $I(V)$ characteristics (cf. Fig. 1c) and current oscillations at high potentials, exactly as expected by the CBM (cf. Section 7).

Since the oxidizing power of the org electrolytes is so important, it is often necessary to bubble the electrolyte with N_2 before use, in order to remove all traces of O_2 dissolved from the air. Of all electrolytes tried, DMSO and DMA produce the most perfect p-macropores(org). There is little doubt that their combination of relatively large oxidizing power and sufficient passivation power supplies the best compromise for etching well-formed p-macropores(org).

2.4. Macropores in p-silicon obtained with aqueous electrolytes

If p-macropores(org) came as a surprise, so did p-macropores(aqu) which were first described by Lehmann and Rönnebeck [60]—after several hundred papers had been published exclusively finding p-micropores(aqu). However, microporous Si is usually produced with electrolytes containing a large concentration of HF (often just 49% HF mixed with an equal volume of ethanol), and at current densities close to the j_{PSL} value of the system, while p-macropores(aqu) are found at current densities much lower than j_{PSL} and for medium to low HF concentrations. Fig. 11 shows some representative species.

The p-macropores(aqu) occupy some region in the parameter space (roughly) defined by the HF concentration [HF] and the current density. While there is a general agreement in the literature that [HF] determines j_{PSL} (although, no doubt, the nature of the additions will play a minor role, too), there are few and seemingly contradictive quantitative data. Lehmann [36] reported an exponential relationship of j_{PSL} on [HF], while van den Meerakker et al. [49] found a linear dependence. The actual data, however, if plotted in the same diagram, are reconcilable as shown in Fig. 12. The figure also contains some predictions from the CB model as to the parameter space of p-macropores(aqu).

The SCR-model may account for these pores to some extent, because they occur at small currents which means that there is still a sizeable SCR that could focus carriers on pore tips and that would provide an impenetrable barrier for holes if the walls between p-macropores(aqu) are completely contained in the SCR [60]. Likewise, diffusion instabilities may favor p-macropores(aqu) to some extent.

Not many properties of p-macropores(aqu) are known at present; nevertheless, we attempt to summarize and generalize as follows.

- The p-macropores(aqu) are rather easily obtained for [HF] < 15 wt.% and $j < 0.05 j_{PSL}$ if nucleation is provided for, e.g. by KOH etch pits.
- Without pre-defined nucleation, an extensive nucleation period may be necessary.
- The walls between p-macropores(aqu) are always rather thin (corresponding to twice the SCR width).
- Lehmann's formula does not apply: there is no defined relation between a, d, and other variables; pores with predefined nucleation always grow in diameter until they almost touch each other.
- Pores with large diameters obtained in this way, tend to have ''cloudy'' tip shapes, cf. Fig. 11b.
- Randomly nucleated p-macropores(aqu), while still keeping pore wall dimensions small, have well defined average diameters with smooth tips and walls (cf. Fig. 11a).
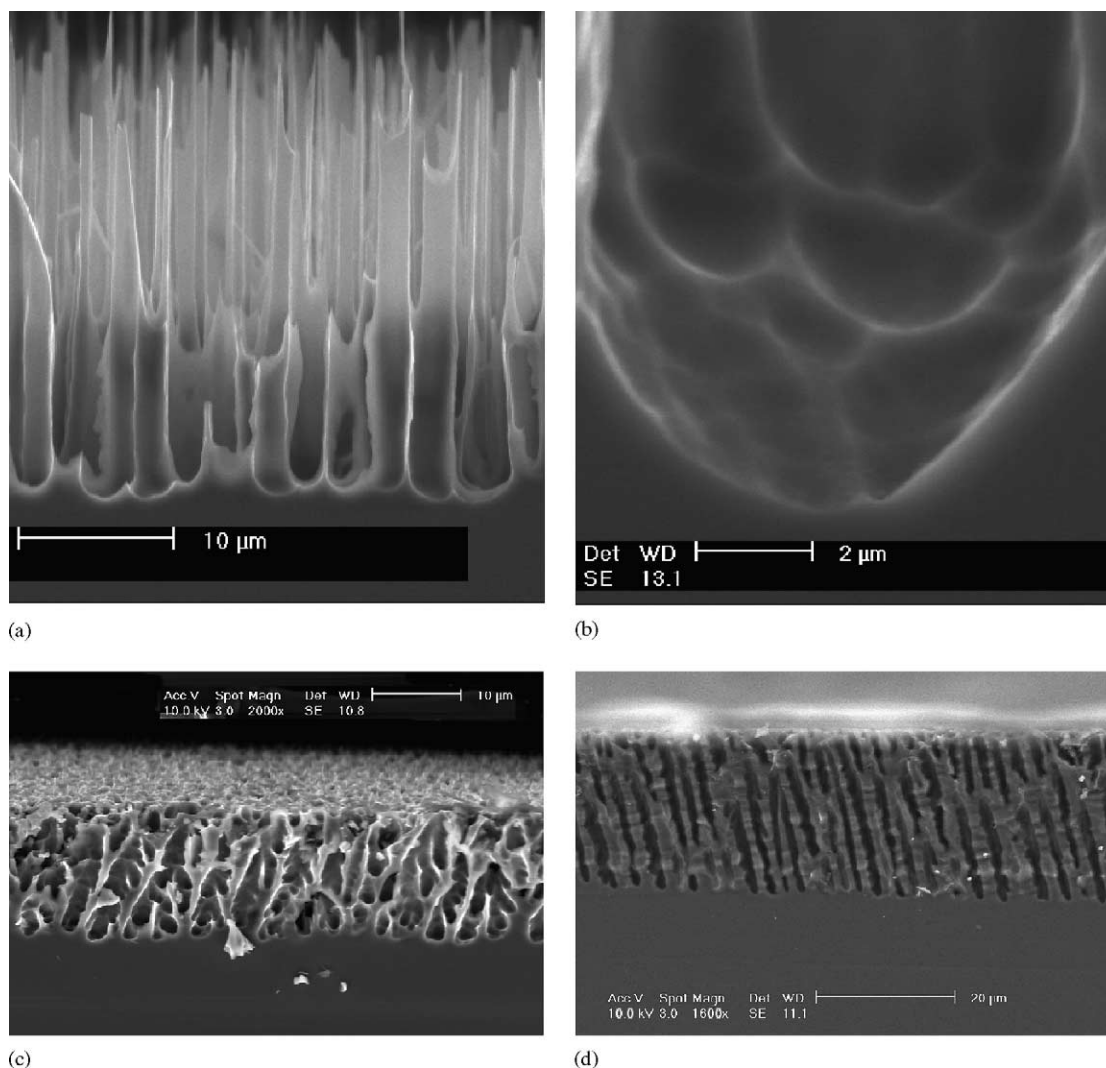
Fig. 11. Some samples of p-macropores(aqu): (a) $10\,\Omega\,cm$; 7% HF, $j = 20\,mA/cm^2$, $j_{PSL} = 90\,mA/cm^2$, random nucleation; (b) as (a), but induced nucleation (hexagonal lattice, $a = 3\,\mu m$); (c) $10\,\Omega\,cm$; 10% HF, $j = 2\,mA/cm^2$, $j_{PSL} = 150\,mA/cm^2$, random nucleation on {5, 5, 12} sample; (d) p-macropores(org) with MeCN (4 wt.% HF) on {1 1 1} for comparison with (c).

- Not much is known about the orientation dependence of p-macropores(aqu); but it appears to be similar to that of p-macropores(org) obtained from electrolytes with small oxidizing power. In particular, p-macropores(aqu) obtained in {1 1 1} Si, are practically indistinguishable from p-macropores(org) with MeCN as electrolyte—cf. Fig. 7c and d.
- The CBM predicts that p-macropores(aqu) occur for currents below the point of inflection on the $I(V)$ characteristics [11].

The CBM has much more to say to the formation of p-macropores(aqu), but since so far no immediate uses have emerged, we will not dwell on the subject and mention it only briefly in Section 7.
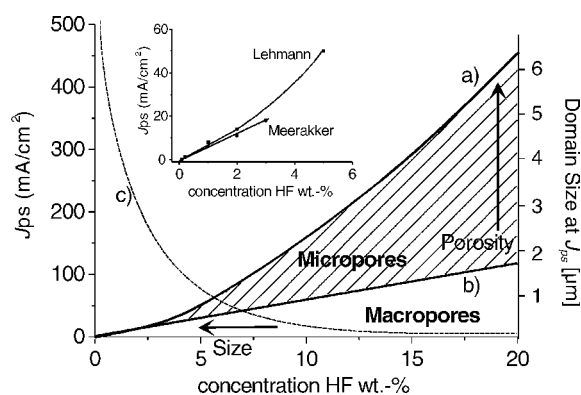
Fig. 12. Parameter space for p-micropores(aqu) and p-macropores(aqu). Curve (a) shows j_{PSL} as described by the Lehmann model [36] and curve (b) as described by van den Meerakker [49]. Curve (c) describes the size of a CB domain. The regions for macropore- and micropore-growth are a result of a semiquantitative consideration of the CB model and may be considered as a prediction. The inset shows measured data taken from [36,49] for low HF concentrations.

2.5. Macropores in n-silicon obtained in aqueous electrolytes using front side illumination

As in the case of p-macropores(aqu), the SCR-model would not necessarily expect well formed macropores if the front surface of n-type Si is illuminated. As mentioned before, n-macropores(aqu/bsi) were actually predicted based on observations with front side illumination; Fig. 13 includes these ''historical'' pictures. Essentially, only conical depressions were obtained that would not be called macropores [17].

Besides a systematic study of Levy-Clement et al. which established the existence of n-macropores(aqu/fsi) [57], nothing else seems to be published about this kind of macropores. In general, three different zones were found [24]: an etch crater, a microporous and a macroporous silicon layer. The morphology of the zones depends strongly on the etch conditions, e.g. charge transferred, doping level, HF concentration, surface orientation. The authors summarized that some of their results are consistent with a depletion layer model while others are not.

Meanwhile, however, new results have been obtained published here for the first time and shown in Fig. 13c and d. Well developed n-macropores(aqu/fsi) oriented in $\langle 1\,0\,0 \rangle$. A totally new result is the observation of n-macropores(org/fsi), similar to the ones obtained in aqueous electrolytes, but with stronger (periodic) branching. The inclined n-macropores(aqu/fsi) shown in Fig. 13f serve to rule out that light penetrating a pore generates carriers at the pore tip and thus promotes pore growth. Considering that a pore is the opposite of a wave guide and will quickly scatter light into the Si, it is unlikely that carriers are generated close to the pore tip. The unavoidable conclusion is that carriers must diffuse from the surface near region where they are generated to the pore tips. While the conical shapes indicate that there is some initial lateral pore growth (especially in the form of branches) in surface near regions, the strong unbranched growth in the depth unambiguously requires some kind of passivation of the pore walls, as concluded in other cases before.

2.6. Macropores in n⁺-silicon obtained in aqueous electrolytes with additions of oxidizing electrolytes

The n^+-macropores(aqu + ox) merit special mentioning (despite their present uselessness) for two reasons: first, they demonstrate that there is still room for new findings within the context of the
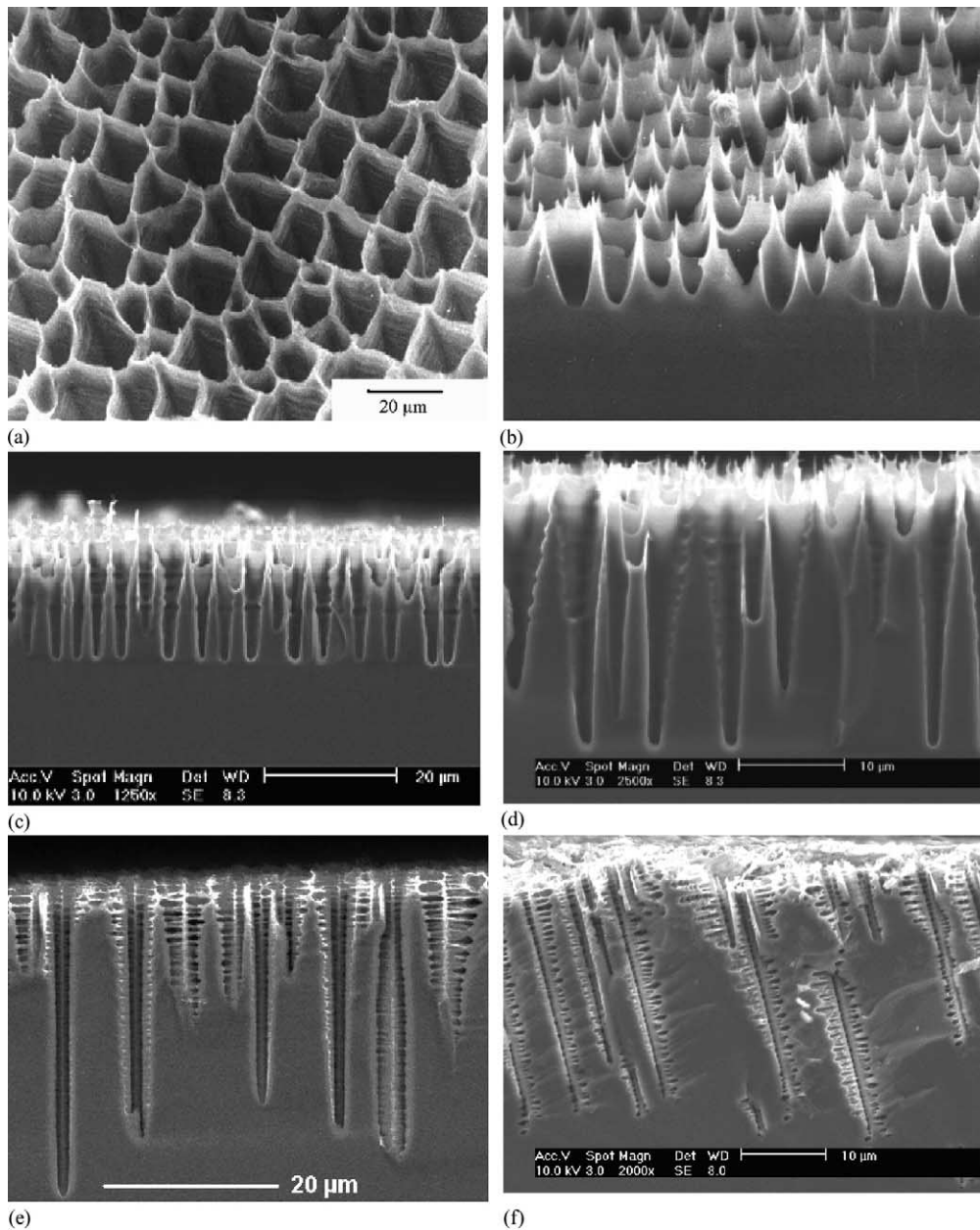
Fig. 13. Various n-macropores(fsi): (a) ''old'' picture from 1985 showing the surface of n-type Si etched in an aqu electrolyte and with front side illumination; (b) cross-section to (a). (c and d) n-macropores(aqu/fsi); (e and f) n-macropores(org/fsi/DMF) on {1 0 0} or {1 1 5}, respectively. For (c)–(f), 3–6 Ω cm samples, 5 mA/cm², 4 V.

electrochemistry of Si, and second, they were found in a systematic experiment on the base of another prediction, this time coming from the CBM.

Until their discovery, it was generally believed that pores in heavily doped Si (of both doping types) would always be mesopores. There was no theoretical justification for this, simply because non of the existing models (with the exception of the avalanche break-through model introduced in 2000 [61]) said anything to n^+-, p^+-pores at all. However, there was much experimental evidence: whatever you tried—mesopores were the result.
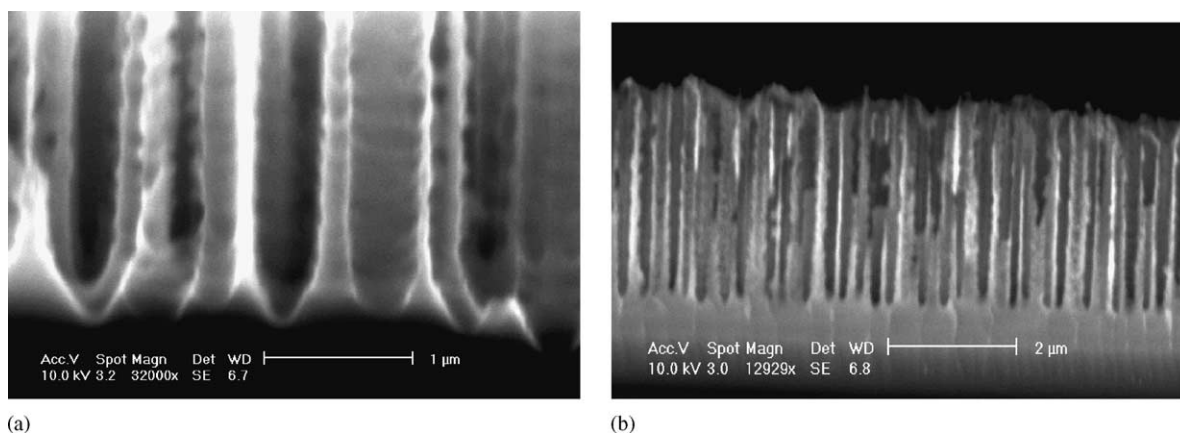
Fig. 14. Macropores in highly doped Si (0.020–0.060 W cm): (a) TMAH addition; (b) CrO$_3$ addition.

The CBM considers mesopores to dominate whenever the formation of SiO$_2$, i.e. oxidation—is weak as compared to direct dissolution. Oxidation, in turn, is weak if the supply of holes is small compared to what the electrolyte can "process" by direct dissolution. Since the maximum direct dissolution current is exponentially increasing with the potential at the Si surface, this condition is always met for heavily doped Si. In this case, the voltage drop across the (very small) SCR is negligible and almost all of the applied potential is available at the Si surface, allowing much larger direct dissolution currents as even p$^+$ Si can deliver.

This leads to the expectation that strengthening of the oxidation by adding strongly oxidizing chemicals to the aqueous electrolyte could supply sufficient oxidation which then would induce macropores.

Indeed, n$^+$-macropores(aqu + ox) could be achieved with several oxidizing ingredients; Fig. 14 shows examples. The most useful oxidizers were CrO$_3$ and TMAH, more details can be found in [34]. However, no p$^+$-macropores(aqu + ox) could be produced with electrolytes that worked for the n$^+$-case.

While applications are not considered at this point, n$^+$-macropores(aqu + ox) demonstrate not only that electrolytes can be "designed" with some guidance, but Fig. 14b gives a hint that this results might be useful in producing macropores at very small pitch values.

2.7. Macropores in n-silicon obtained with organic electrolytes and back side illumination

This case, first reported in 2000 [22] produced very unexpected results which, in the view of the authors, might prove to be of considerable importance for the general understanding of the electrochemistry of Si and its possible technical uses. Using an electrolyte that produced rather perfect p-macropores(org), its application to n-type Si with back side illumination resulted in pores with several new features, cf. Fig. 15.

The few experiments performed so far with n-macropores(org/bsi) yielded a wealth of new data. The general observations were as follows.

- The pores are wildly branched (in $\langle 1\,1\,3 \rangle$ directions) and frequently issuing forth from two-dimensional cavities bounded by {1 1 1} planes on one side (called "wings" in [34]; cf. Fig. 15b).
- Besides n-macropores(org/bsi) and "wings", mesopores were often present at the same time (see Section 4).
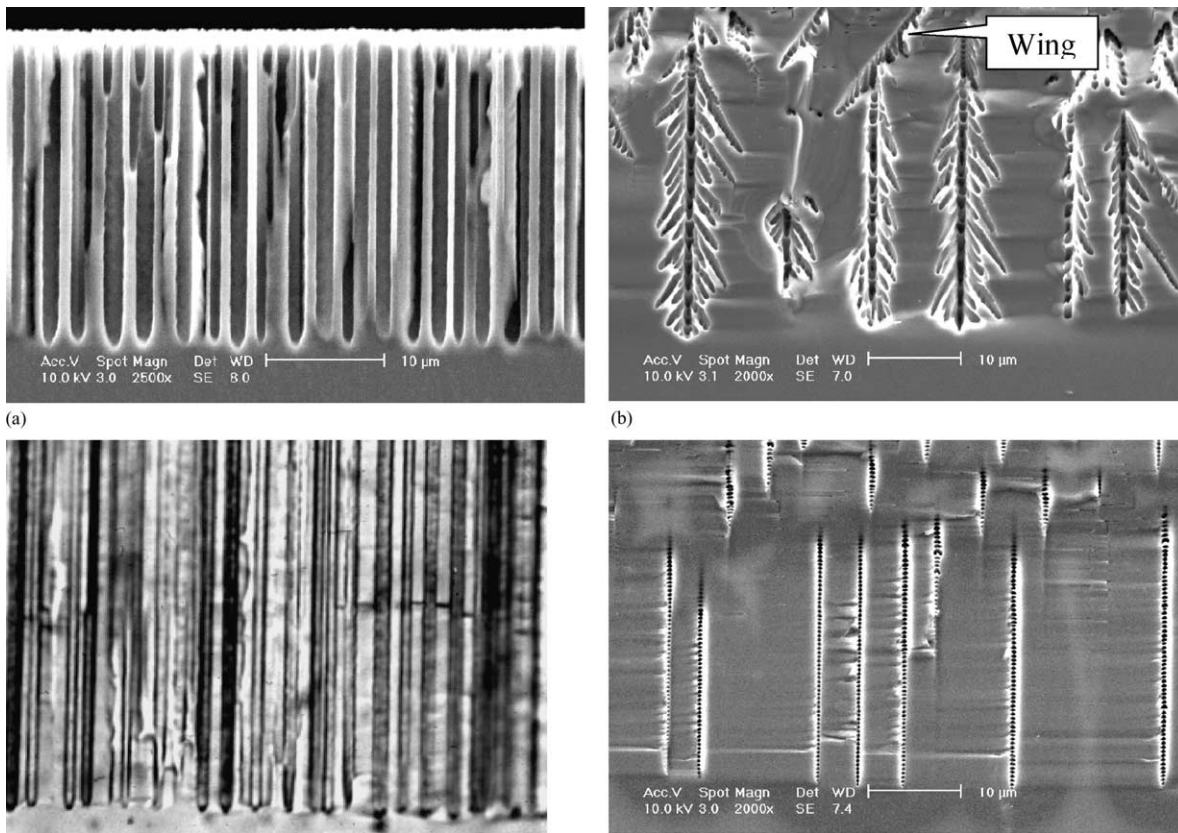
Fig. 15. Comparison of p-macropores(org) and n-macropores(org/bsi) for similar etching conditions (10–20 Ω cm samples, $j = 2$ mA/cm^2, $U = 2$ V): (a) p-macropores(org); (b) n-macropores(org/bsi) without superimposed ac current; (c and d) as (a) and (b) but with an ac current (33 mHz, amplitude $= 0.2\ j$) superimposed on the etching current j.

- The n-macropores(org/bsi) respond in an extremely non-linear fashion to ac currents super-imposed on the etching current: whereas for frequencies below 33 mHz no visible changes occur, at 33 mHz the n-macropores(org/bsi) assume a regular shape without side pores and contain diameter modulations corresponding to the current modulation (Fig. 15d). This can only be described as a kind of chaotic resonance. The same current modulation with p-macropores(org) produced no noticeable effect (Fig. 15c).

Only few data about n-macropores(org/bsi) are available at present and no pore formation model besides the CBM has attempted an explanation so far. Of course, just considering the morphology, the SCR-model would have expected that perfect pores should result, given the additional stabilizing influence of the SCR and carrier focussing in a system that already produced rather perfect p-macropores(org). The observed resonant behavior at present seems to be beyond the reach of the ''static'' models (all except the CBM).

The resonant behavior of n-macropores(org/bsi) offers a new variable for controlling the growth of all pores in Si that has not been considered so far: modulations of the current, the voltage, or the light intensity with the right frequency and amplitude, may stabilize pores that would be unstable otherwise. While this new feature might be useful for applications, a much better understanding of the dynamics of pore growth is necessary for its employment.

3. Applications of macropores

3.1. General remarks

Macropores offer a number of attractive features for many kinds of applications. A listing includes:

- extremely large aspects ratios (length/diameter) of >600 for diameters in the 1 μm region;
- defined geometries (arrays) are possible—periodic, periodic with defects, or aperiodic—the only limitation being that the average pore density should be constant;
- large porosities and thus large volume to surface ratios are possible;
- large areas can be homogeneously etched due to the supreme homogeneity of Si wafers;
- full compatibility with Si technology.
   There are, however, also some difficulties in employing macropores for products. These may be listed as follows.
- Si technology is often needed, i.e. a cleanroom with some standard processes like lithography, oxidation, Si_3N_4 deposition—in other words an expensive infrastructure for research and development.
- Etching macropores on large areas (e.g. on a 200 mm wafer), while certainly possible, is neither easy nor (initially) cheap.
- While ''perfect'' n-macropores(aqu/bsi) are possible, they occupy only a tiny area in the total parameter space as outlined in Section 2. Abandoning this area in search of features not attainable there, will quickly incur a ''black art'' component, not easily accepted for product development.

Applications are now emerging in many areas, where three qualitatively different fields might be distinguished: microelectronic and mechanical systems (MEMS), optics, and ''surface''; with ''surface'' meaning the use of large surface to volume ratios without much additional patterning for various projects. There is some overlap and we include all applications in the MEMS category that need some kind of structuring beyond just using porosity.

So far, almost exclusively n-macropores(aqu/bsi) were used and in what follows this type is meant whenever simply mentioning ''macropores''.

3.2. Applications to MEMS

One of the earliest applications of macroporous Si was pioneered by Ottow et al. [62,63] who used densely spaced regular macropore arrays as a kind of substrate into which deep three-dimensional structures on a larger scale were made. While this ''Ottow''-process is not without some sophistication, in essence the raised areas were covered with a lithographically structured mask and the highly porous Si in the unmasked areas was etched off. Fig. 16 shows early structures obtained in this way; meanwhile the process has been perfected and is routinely employed for photonic crystals (see later and Fig. 19).

A particular innovative use of macropores is in the area of ''Brownian motors or pumps'' [48]. Essentially, involved thermodynamics show that Brownian motion *plus* some asymmetric field can achieve what Maxwells demon cannot: sorting particles according to type or size [64]. In the variant using macropores pursued by the Halle group [65], a membrane containing macropores with a saw-tooth like cross-section separates two reservoirs with particles of two different sizes suspended in some liquid. Pulsing the pressure should pump one kind of particles to the left and the other kind to the right. As mentioned before, obtaining the controlled diameter variations of the macropores was
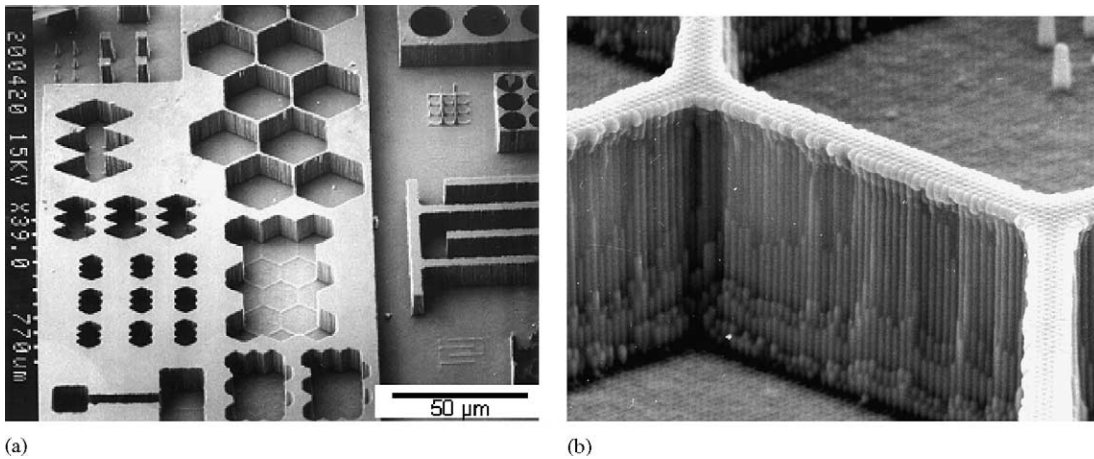
Fig. 16. Structures with large aspect ratios obtained by the ''Ottow technique'' [62,63] from macroporous substrates (early development stage): (a) overview, (b) detail from the hexagonal array.

not as easy as could be expected in most formation models, but Müller et al. [48] did finally succeed in producing suitable membranes and are currently trying to demonstrate Brownian pumping. An example (with a comparison to pores in GaAs) is shown in Fig. 17.

In this application like in many other, it is necessary to have pores that completely traverse the Si substrate; something that cannot be achieved by etching alone. The n-macropore(aqu/bsi) growth will always stop if the pore tip approaches the sample backside. This is understandable because holes can no longer diffuse to the pore tip if the space charge region occupies the total volume of Si between the pore tip and the sample backside. While for all other kinds of macropores this limitation has not been experimentally demonstrated, it must be expected to occur as well. In any case, macropores that would ''grow out'' on the backside are not desirable because of subsequent
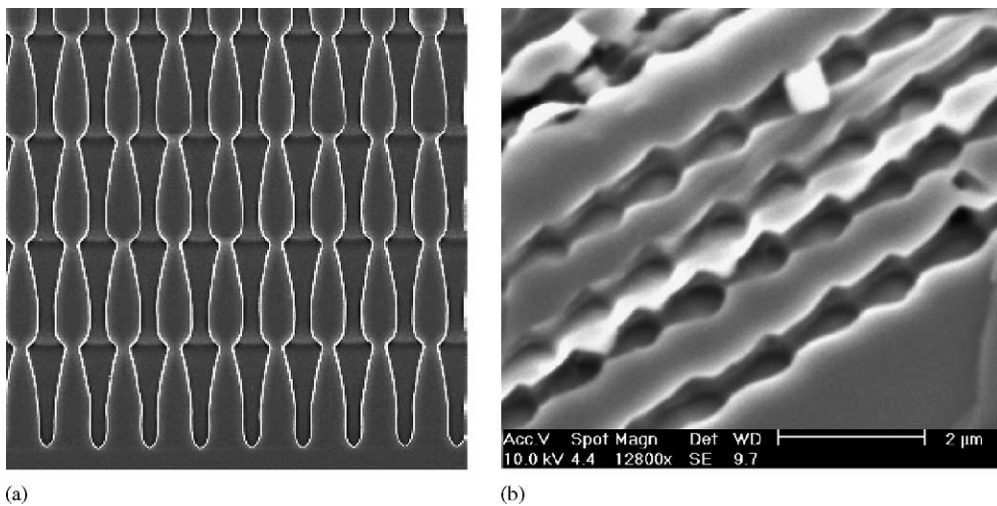

Fig. 17. (a) Macropores in Si with intentionally modulated pore cross-section intending a saw tooth shape (the distance between the center of the pores is 4.2 μm; courtesy of Müller et al. [45]). (b) Macropores in GaAs without intentional diameter modulation. A saw-tooth shape evolves naturally demonstrating the close link between pores and oscillations (from [96]).
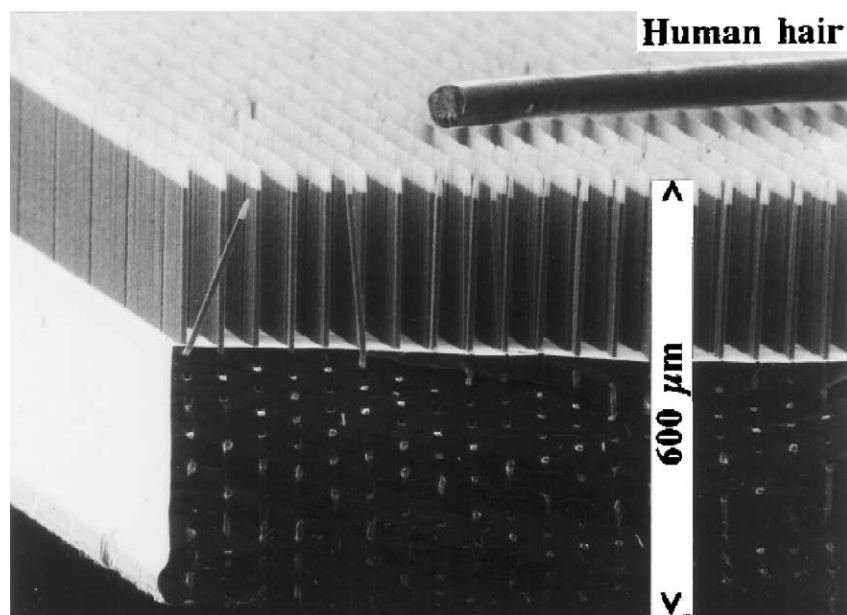
Fig. 18. Macropore array filled with lead taken from [66]. In the upper half of the sample, the Si was removed and the lead wires are exposed.

electrolyte leakage (or, in the case of electrolytic double cells, short circuits between the back- and frontside). It is therefore necessary to remove parts of the backside by mechanical polishing or plasma etching; a delicate operation for highly porous samples.

A novel use for macropores are X-ray filters. In medical X-ray imaging, all inelastically scattered photons reaching the film blur the image. (Consider a simple analogy: a strong light source will transmit some light through your hand. Without the inelastically scattered light, i.e. looking only at the directly transmitted light, you could see the bones.) A filter highly transparent to X-rays propagating along the optical axis, but not transparent in all other directions, could considerably increase the contrast of weakly scattering objects (encountered, e.g. in mammography). Recent work by Lehmann and Rönnebeck [66] used macropores filled with lead to produce such a filter. In this case, it may be necessary to use an aperiodic pore array with constant pore density to avoid Moirée effects with the periodic diode array in the CCD cameras universally used in X-ray devices. Fig. 18 shows an example of the structures achieved. If fully optimized, the filter could reduce the X-ray dose by a factor of three without loss of resolution, or allow better images, respectively.

Macropores are also envisioned to be useful for chemical microreactors. At least one group [67] is working on this subject and at least one patent application is on record [68]. The large surface of porous silicon offers unique possibilities to synthesize specific chemicals in a microformat at chip dimensions. The reactions would be catalyzed by enzymes coating the pores; this is generally possible as demonstrated in [67]. Bengtsson et al. made a particular interesting approach to this topic by etching macropores in the wall of trenches pre-fabricated on {1 1 0} silicon. The trenches direct the flow of the reacting species; they were etched anisotropically with alkaline solutions and therefore have rectangular cross-sections. The macropores are coated with (immobilized) enzymes and the reaction rate is greatly enhanced by the increased active surface area. Highly efficient biocatalytic microreactors are obtained if the macroporous matrix is optimized with respect to pore geometry, morphology, and depth.

A relatively new issue for macropore applications is biotechnology [69]. Looking at regular macropore arrays, it is suggestive to use them for "biochips". A biochip, loosely speaking, is a matrix of tiny test tubes in a regular array each of which is coated with a biochemical that reacts only with specific molecules or DNA sequences. Absence or presence of a reaction can be monitored optically (e.g. by luminescence or IR absorption) or electronically, and the position in the matrix identifies the chemicals present in the solution to be analyzed. This allows for quick and fully automated detection of thousands of molecules simultaneously. Besides suitable pore arrays, technologies for the coating of the pore walls and some suitable detection scheme must be developed; efforts in this direction are under way. Work in the Infineon laboratories has progressed to a point where first prototypes have been made and the technique may see product applications in the near future [69].

Sensors based on optimized macropore arrays have been under development for some time. In particular, Angelucci et al. [70] developed a sub-ppm benzene sensor for air quality monitoring. The key part of the device is a permeable macroporous silicon membrane, a few tens of microns thick, and with the pore walls coated by a semiconducting SnO_2 film. This film changes its resistivity in the presence of benzene (and other gases) and the large surface together with the optimized gas flow pattern through the pores allows extreme sensitivities. As stated before, a special process step is needed to open the pores at the back end of the specimen.

Kleinmann et al. [47] developed arrays of scintillating guides for digital X-ray imaging systems. Such scintillating guides have to be compatible with a special CCD cell spacing. Scintillating guides were etched electrochemically in n-type silicon. The pores were filled subsequently with a scintillating material.

Astrova et al. [71] studied the diffusion of boron and impurities into the walls of macroporous silicon with applications for power devices in mind. However, little has been published, to this issue although there is an old patent [72]. Of course, the general structure of the X-ray filter shown in Fig. 18 could also be used for a novel power device: the metal fingers, separated from the Si by a thin dielectric layer, could be used as gates, surrounding each finger with a depletion zone of variable depth. Current flow perpendicular to the filled pores then could be modulated by the voltage on the metal fingers akin to the grid voltage of an electron tube modulating current flow from the cathode to the anode.

So far, it has been very difficult if not impossible to produce macropores in structured areas without underetching the mask. However, recently Starkov et al. [73] showed that a particular combination of photoresists and etching conditions produced macropores with a depth of up to 100 μm without any underetching of the mask.

Finally, first possible uses for the trenches (Fig. 6) are emerging. Xie et al. are working on the integration of analog and CMOS devices in one chip which calls for dielectric insulation and complete metal encapsulation of the analog part of the chip. While the first task could be performed by utilizing microporous Si, the latter task is more difficult to tackle. Etching a trench around the analog portion which is subsequently filled with metal may be an attractive candidate for this task; the technique is presently evaluated.

3.3. Large surface to volume ratios

Lehmann et al. developed a capacitor based on macroporous silicon. Essentially, macropores (or mesopores) are etched into a Si substrate and coated with a standard high-quality dielectric, usually a few nm thick ONO (oxide–nitride–oxide) layer. Deposition of (highly doped) poly-Si provides the second electrode. Specific capacities of 4 μF V/cm^3 are possible, comparable to Ta_2O_3 capacitors,

and all other properties, especially the resonance frequency, are better then all competitors. The porous Si capacitors are naturally fully compatible with Si technology and, due to their extremely good dielectric, of very high quality.

The process has been developed to a production level, but the product has not yet been scheduled for mass production.

It has been realized rather early that macroporous layers with relatively shallow pores and preferably with diameters that are large at the surface and decrease with depth are ideally suited as anti-reflection layers for solar cells or for "black-body" emitters with optimized IR radiation [74]; such layers could be made most easily with-macropores(aqu/fsi), Fig. 13b) shows an example. However, since macropores in p-type Si were discovered much later and n-type Si is not used for solar cells, not much came of it. Note in this context that the use of microporous (or mesoporous) Si as an antireflection coating predates the discovery of its essential properties [75].

More recently, Levy-Clement and coworkers extensively studied the use of p-macropores(org) as antireflection layers on multicrystalline solar cell substrate material [76,77]. While good results were obtained, the approach is somewhat hampered because of unfavorable pore geometries for grain orientation around {1 1 1}. For the use of microporous Si as antireflection layer see Section 5.2.

Macroporous layers etched from the backside into defined areas on a Si substrate may also be used either as a "low k" material, i.e. as regions with strongly reduced dielectric constant (DK), or as "low σ" area, i.e. with large transverse resistance. This can and has been used, e.g. for (relatively large) integrated inductors (spiral coils) which would suffer eddy current losses increasing with the square of the frequency if used on bulk Si.

Macroporous arrays in Si could also be used as a template for the production of "metallic barcodes as described in [78]. In this case, a succession of different metals is used to fill pores; after dissolution of the template (which was porous Al_2O_3 in [25]), submicrometer metal rods with optically identifiable "stripes" are obtained which have many uses as a kind of label in, e.g. biotechnology.

3.4. Macropores and optics

The most prominent and unique application of macropores is in the area of photonic band-gap (PBG) materials, so-called photonic crystals [79,80]. In essence, photonic crystals consist of periodic variations of the index of refraction on a scale matched to the wave length of light, i.e. in the sub-μm region. In a loose but rather fetching analogy, a photonic crystal does to light waves what a real crystal does to electron waves. In particular, an optical band-gap may develop, not allowing the propagation of light in the relevant energy region, and states in the band-gap may be introduced by defects in the photonic crystal, that allow "processing" of light similar in some (but not all) respects to semiconductors. Photons, e.g. may only propagate along one or two dimensional defects, or may even become localized at zero order defects. While photonic crystals offer exciting research fields and a host of new applications, they are not easy to make.

The best two-dimensional photonic crystals are actually obtained by optimized macropore lattices, as first realized by Grüning et al. [81]. A complete optical band-gap was observed in all directions perpendicular to the pores. Since then, complex photonic crystals, including "macro"-structuring by the "Ottow" technique explained above and controlled defects, have been made by Birner et al. [82], Fig. 19 shows an example. Unfortunately, it proved exceedingly difficult to reduce the lattice parameter to dimensions below about 0.8 μm. The Halle group meanwhile
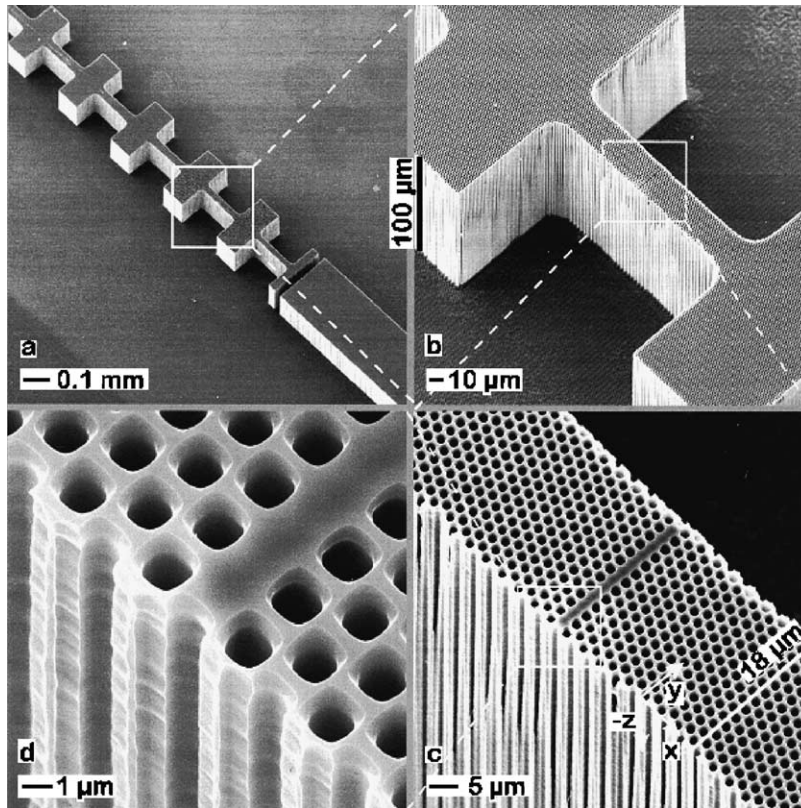
Fig. 19. (a–d) Two-dimensional photonic macropore crystal with a line defect (from [78]).

succeeded in this task, but only by using a highly doped Si crystal especially grown by a float-zone technique [83].

While macropore lattices are perfect for two-dimensional photonic crystals, three dimensional pore crystals are harder to produce. One option is the exploitation of the peculiar $\langle 1\,1\,3 \rangle$ growth direction. Under favorable conditions macropores grow in all three symmetrically equivalent $\langle 1\,1\,3 \rangle$ directions if seeded on $\{1\,1\,1\}$ samples. If the nucleation is induced in a properly aligned hexagonal lattice, three pores will meet at one point which then acts as nucleus for a new three-fold; a three dimensional pore crystal with an orthorhombic symmetry (preferred for photonic crystals) results. The results of a first experiment along this line is shown in Fig. 20.

There are, however, more ways to produce three-dimensional photonic crystal structures by pore etching. In particular, a macropore lattice in microporous Si with a defined porosity modulation, or defined diameter modulations of the macropores in a photonic crystal, may introduce the third dimension in a way sufficient for some applications.

Macropore arrays have also interesting optical properties in the pore direction. Very roughly speaking, photons with wave lengths smaller than the pore diameter pass through, others are blocked. While it is actually more complicated than that (total reflection and diffraction effects at small apertures must be considered), the general behavior is that of a (very good) filter for short wave lengths, completely blocking longer wave lengths, cf. Fig. 21. Lehmann et al. produced and described such a filter based on n-macropores(aqu/bsi) [84]. In contrast to Bragg or glass filters the light is not transmitted in the matter but in the medium inside the pores, i.e. in air (or possibly vacuum), which is advantageous for many applications.
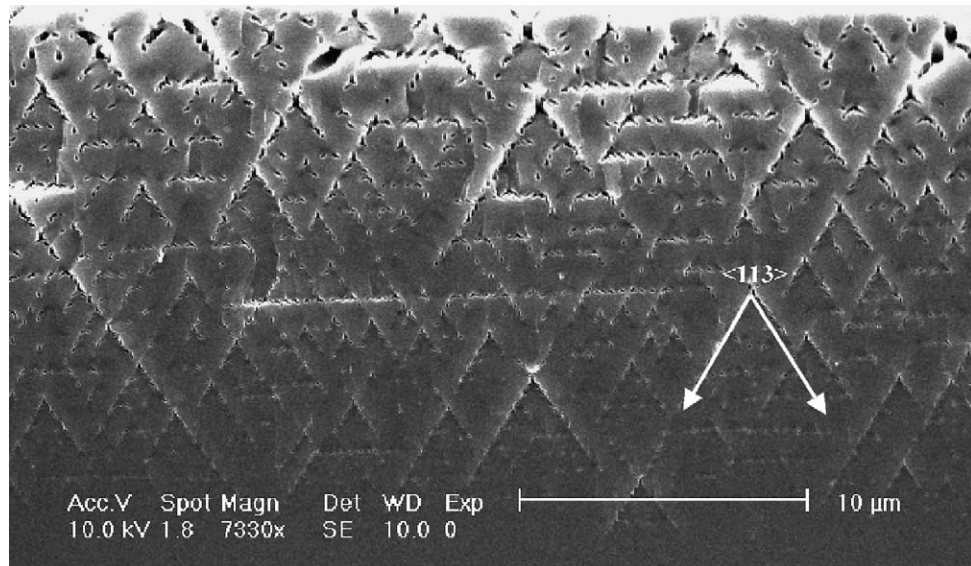
Fig. 20. First three-dimensional photonic crystal expressed in a intersecting ⟨1 1 3⟩ oriented macropore lattice on {1 1 1}.

Finally, optical applications may profit from macropores in an indirect way, too, by using cheap variants of the ''Ottow'' technique described above to produce moulds for casting microlenses. Essentially, producing a deep circular depression would already be sufficient because a layer of glass bonded to the Si mould would extent semispherically into the depression, driven and stabilized by surface tension [85]. Using p-macropores(org) grown only in unmasked areas (with optimized underetching) in connection with the trenches obtained under these conditions, may be the way to success.
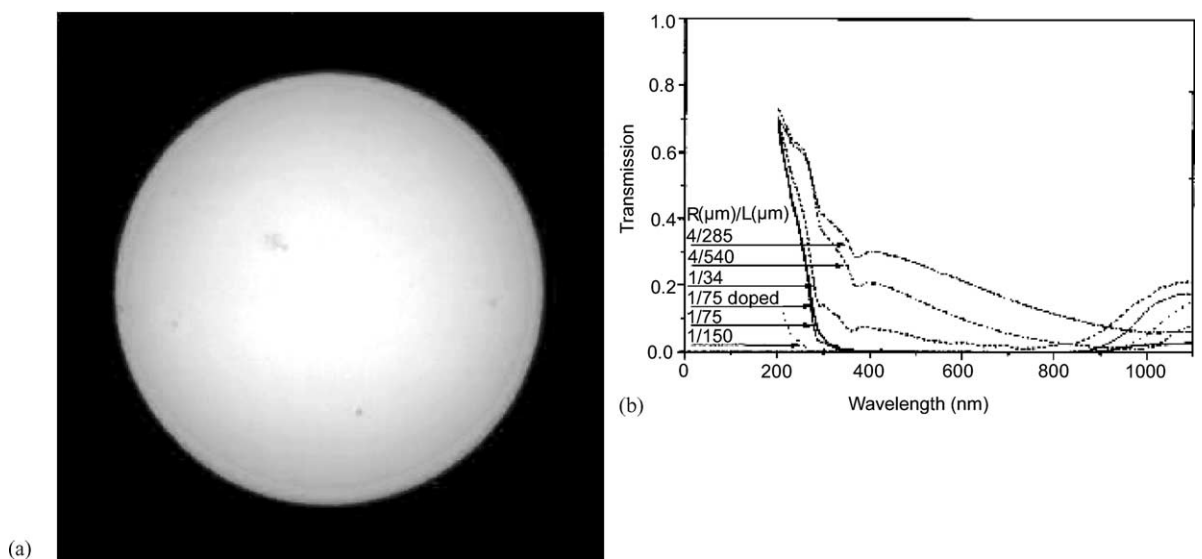

Fig. 21. (a) The sun viewed through a deep blue and UV transparent macropore filter. The original picture is deep blue; sunspots are clearly visible. (b) Transparency curves of various macropore UV transmitters. R and L denote the pore diameter and depth, respectively. Courtesy of V. Lehmann; cf. [79].

4. Mesopores

4.1. Formation and appearances

By IUPAC definition, mesopores are all pores with $10\,nm < d < 50\,nm$, but, as stated before, this definition is too limited to be of much value. We will therefore use the following list as a working definition of mesopores; it coincides roughly with the geometric definition.

Mesopores are obtained for the following configurations.

1. Etching of highly doped Si in aqueous electrolytes always produces n^+/p^+-mesopores(aqu); Fig. 22a shows an example. No light is required in the case of n^+ Si because avalanche breakthrough is easy and enough current will be produced even at small voltages. Lehmann et al. conducted a detailed study of these kinds of mesopores [61] to which the reader is referred.
2. Etching of moderately or low doped n-type Si in the dark produces ''break down'' (bd) pores (at voltages that might be as large as 100 V) which must not only be counted as mesopores by the geometric definition, but also within the frame work of the CBM. This kind of mesopores we denote n-mesopores(aqu/bd); Fig. 22b shows an example.
3. Etching of highly doped Si in organic electrolytes produces n^+/p^+-mesopores(org) which are quite similar to their n^+/p^+-mesopores(aqu) cousins [10,34], but may occur already at lower doping levels. While little work has been devoted to these pores, it appears that weakly oxidizing org electrolytes tend to encourage mesopore growth while strongly oxidizing electrolytes even allow macropore formation; Fig. 22c shows an example.
4. The n-mesopores(org/bsi) appear together with n-macropores(org/bsi); Fig. 22d shows examples.
5. Mesopores are found on occasion inside macropores, i.e. the macropores are filled with mesopores. This is actually just a special case of p-mesopores(org) obtained in weakly oxidizing electrolytes as discussed in Section 2.
6. Mesopores are on occasion observed to issue forth from macropores that stopped growing [86]; a particular tricky case for pore formation models; cf. Fig. 23a.

As seen from the examples provided in Figs. 22 and 23 and from numerous published and unpublished sources, mesopores have some common characteristics (not without occasional exceptions, however).

- They only grow in $\langle 1\,0\,0\rangle$ directions [34] and since they are usually branched the branches are at right angles to the main pore. In instances where this seems to be not the case (e.g. Fig. 22c), the branches do not have a well defined geometric shape [61].
- Whenever mesopores assume some defined geometric shape (which seems to be tied to low current densities), it consists of connected octahedra as shown in Fig. 23b and c.
- At higher current densities the mesopores are still growing in $\langle 1\,0\,0\rangle$ directions, but the geometric shape of the branches is lost; they appear ''cloudy'' as illustrated in Fig. 22c.

As in the case of macropores, some possible mesopore configurations are missing since they have not been investigated so far. This includes n-mesopores(org/bd), n-meso-pores(org/fsi), and—as a prediction of the CBM—n-mesopores(org/bsi) for weakly oxidizing organic electrolytes. Time will tell.

While there seems to be no conceptual problem with the formation of n-mesopores(aqu/bd)—after all, if avalanche break down is the only source of holes, the resulting pores must be small to allow high field strengths at the tips—the situation is not quite that clear: Why are n-mesopores(aqu/bd) always heavily branched (their counterparts in III–V semiconductors tend to be perfectly straight)? If the
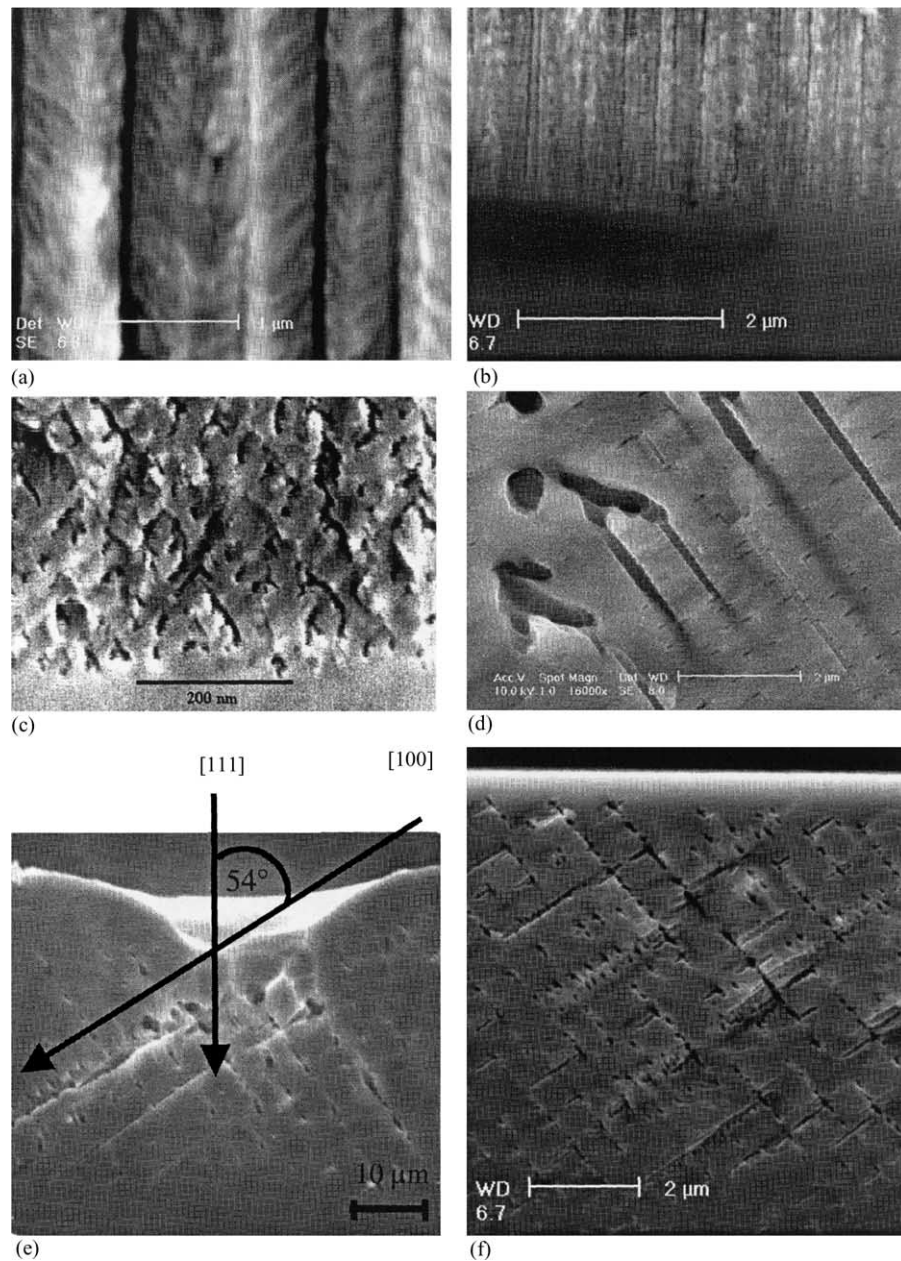
Fig. 22. Various kinds of mesopores: (a) n$^+$-mesopores(aqu/bt), low current densities (2 mA/cm^2); (b) p-mesopores(org/ MeCN); (c) n$^+$-mesopores(aqu/bt) at high current densities (50 mA/cm^2), from [41] (courtesy of V. Lehmann); (d) n-macro(org/bsi), $\langle 2\,3\,3 \rangle$ substrate; (e) n-mesopores(aqu/bt), $\langle 1\,1\,1 \rangle$ substrate; (f) n-mesopores(org/DMF/bt); $\langle 1\,1\,1 \rangle$ substrate.

pores are close enough to each other (which they usually are), there should be no sizeable electrical field between the pores and thus no inducement to branching. Moreover, there is no good reason why n-mesopores(aqu/bd) exclusively produced by avalanche break down should not always grow perpendicular to the sample surface, something they emphatically do not (again in contrast to their III–V cousins) as shown in Fig. 22e and f.
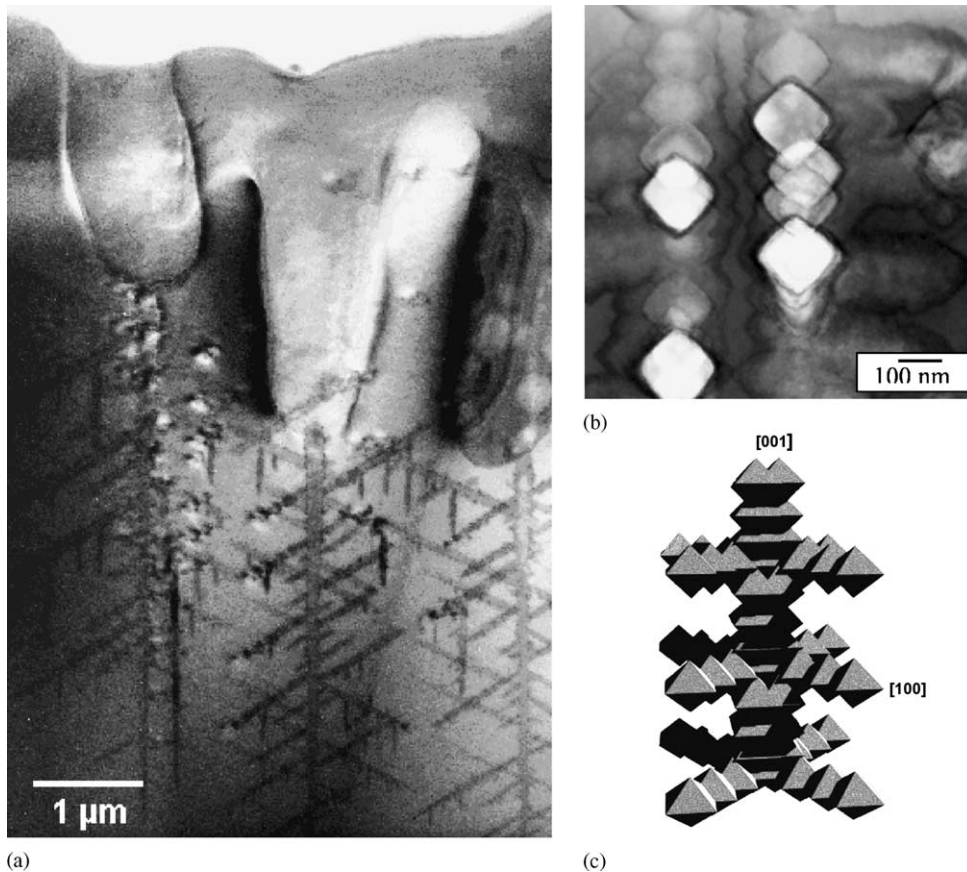
Fig. 23. (a and b) TEM micrographs of macropores with mesopores in n-type silicon (bsi, aqu) from [81]; (c) schematic view of a mesopore.

All things considered, there is no convincing model for the formation of mesopores at present, although the CBM has some suggestions (see Section 7).

As far as the authors know, there has been no attempt to grow mesopores from pre-defined nuclei. While this is simply due to the difficulties in obtaining lithography well below 0.1 μm for dense arrays of n-mesopores(bt), there is no particular reason not to try n-mesopores(bd) in some version at larger spacings for any electrolyte.

4.2. Applications of mesopores

The first large-scale commercial product based on pores in Si actually uses mesopores for producing silicon on insulator (SOI) wafers. The ingenious Epitaxial layer TRANsfer (ELTRAN[TM]) process from CANON[TM] [7] first produces a "normal" mesoporous layer of a few μm thickness, followed by a layer with very large porosity by changing the current density in situ. After an H_2-anneal that closes the pores on the wafer surface, an epitaxial Si layer (which will be the functional layer) is deposited. Next the wafer is bonded to an oxidized second wafer. A fine water jet splits the wafer stack along the mesoporous layer with the large porosity—it is like opening a zipper. Finally, a second anneal smoothes the surface obtained and the result is a SOI wafer with a very high quality Si layer on thermal SiO_2.

A similar process was investigated for solar cells by a Japanese company [7] and two German groups [87,88]. Again an epitaxial layer of about 25 μm is grown on a highly porous layer which has been annealed to close the top porous layer. The solar cell is produced on the "thick" wafer and active solar cell structure together with the bulk silicon layer of 25 μm is afterwards lifted off by breaking the highly porous structure. This technique allows to produce thin solar cells with efficiencies up to 15%.

Note that on occasion the mesoporous layers employed are referred to as "microporous". While this is not necessarily wrong on the base of the formal 10 nm limit dividing micropores and mesopores, the ELTRAN™ process seems to employ mesopores—judging from the data given in [89].

This may also be the reason why mesopores are rarely mentioned in the context of applications but often treated under "micropores". In general, it appears likely that mesoporous layers can be used in many cases where microporous layers "work", too. Sensors, Bragg reflectors, waveguides, multilattices, biological applications and sacrificial layers have also been developed (possibly not always consciously) on mesoporous silicon, too [4,5]. In many cases where the lack of luminescence is not detrimental, mesoporous structures are to be preferred because they have a better mechanical stability in comparison to micropores.

5. Micropores

5.1. Some general remarks

Micropores and their possible applications have been covered in detail elsewhere [6–8] and this chapter will be brief accordingly. In particular, we will not cover the luminescent properties of microporous Si or applications that were envisioned and investigated (but never used in production) before the discovery of the luminescent properties of microporous Si, e.g. the "FIPOS" process (short for "full isolation by oxidized porous silicon"), cf. [90].

Generally, groups working with micropores use aqu electrolytes with large HF concentrations for two reasons: (1) microporous layers grow rather rapidly and uniformly and (2) their porosity is high (porosity tends to increase with the HF concentration and the etching current [36,49]). If the current and/or the HF concentration are too small, macropores(aqu) will result.

Both doping types of Si are being used, n-type Si may require some light or larger voltages, but no distinct difference in micropore properties have been reported. For heavily doped Si, mesopores will result under conditions that otherwise produce micropores. This necessitates that there is some transition from micropores(aqu) to mesopores(aqu) if the doping level is increased, and another transition from micropores(aqu) to macropores(aqu), if the current and/or the HF concentration are lowered. By inference, there must be a transition from mesopores(aqu) to macropores(aqu)—what would be needed is some kind of phase diagram as shown in Fig. 12, augmented by a third axis for the doping of the Si.

No model can explain micropore formation satisfactorily. While quantum wire effects seem to be necessary, they only could account for the distance between micropores (which must be so small as to produce quantum wire effects) but not for the diameters.

While until recently only p/n-micropores(aqu) have been observed, according to the CBM it should be possible to obtain p-micropores(org) too, if the organic electrolyte has sufficient oxidizing power. This is indeed the case, with a Formamide based org electrolyte (cf. Table 2) and $j = 2$ mA/cm^2, p-micropores(org/FA) were obtained for the first time. That the pores were indeed micropores

and not mesopores (which is hard to distinguish with a SEM alone), was shown by their strong luminescence in the yellow-orange and even blue regime (cf. Fig. 26d).

5.2. Applications of micropores

Following the discovery of the peculiar optical properties of microporous Si by Canham [1] and Lehmann and Gösele [2] in 1990, the application focus was on optoelectronic devices based on Si, and a large number of electro-luminescent (EL) devices has been presented, cf. [91]. Most of them consist of a microporous layer with a contact layer on top. Various materials have been used for contacts, e.g. thin metals like Au, indium tin oxide (ITO), silicon carbide and conducting polymers [92].

However, while working EL devices based on microporous Si have been demonstrated [91], stable and strong EL has not been achieved despite large-scale efforts. After ∼10 years of research the consensus seems to be that the stability of PL and EL is not a trivial problem. The most promising approach to overcome this problem might be the grafting of special molecules on to the microporous Si surface [93].

Bragg reflectors and Fabry–Perot filters have been realized by a modulation of the PS porosity. These applications are based on the variation of the optical properties with the porosity of the microporous (or mesoporous) films. The Jülich group first showed that multilayers with controlled variations of the porosity and microstructure can be obtained by varying the doping concentration, or by varying the etching parameters (mostly the current density) [94]. Superlattices can be formed in this way which may be used, e.g. as high-quality Bragg reflectors, Fabry–Perot filters, wave guides, or antireflection layers [8]. If microporous multilayers are grown on a substrate with a textured surface, a three-dimensional structure results with possible applications for photonic crystals [95].

Sensors based on microporous silicon use both the large surface to volume ratio of the microporous layer and the optical properties of this material. Since the Si surface is always covered by a thin oxide layer (after sufficient exposure to humid air) as-grown microporous Si is rather stable. The stability can be enhanced considerably, however, by a condensation reaction with alkoxy- or chlorosilanes to produce a new Si–O–Si [96].

If there is a reaction between the silicon and the gas to be detected, the process is generally irreversible. Sailor, e.g. used this for the detection of HF gas by monitoring in situ the dissolution of oxide in PS based interferometers as an irreversible process.

If there is no reaction, the process is reversible and it can be used for continuously monitoring gas concentration. Since the adsorption properties are different for different molecules, so is the charge state of the surface—adsorption induces specific changes in the resistivity (transduction mode of a sensor), of the photoluminescence, and of the reflectivity; all of which can be used for sensor purposes. In particular, the condensation of molecules inside the pores can lead to quenching of photoluminescence by energy or electron transfer. Even an ''artificial nose'' able to detect several gases simultaneously has been demonstrated [97].

Microporous Si is a splendid sacrificial layer and of potential value for MEMS fabrication. Free standing silicon structures, e.g. can be formed by anodizing and selective removal of the microporous silicon formed underneath a silicon membrane [98]. Presently, however, it appears that no product based on this application is available on the market.

It is of some historical interest to note that microporous Si was the key ingredient in the so-called ''FIPOS'' process mentioned above which used the selective formation of microporous Si (only n^+ wells containing a p-region turned into microporous Si during anodization) and its far higher rate of oxidation to produce a p-type region fully embedded in oxide [90].

Canham reviewed porous silicon uses as an active biomaterial [99]. Essential properties are that highly porous silicon surfaces are compatible to and biodegradable in the human body. Living neurons have been cultured on microporous Si [100] and the tissue compatibility of PS has been demonstrated. Microporous Si as a biomaterial thus offers a new and dynamic field of research with important potential applications [101].

A new way of using microporous (and/or mesoporous) Si as antireflection coating for solar cells has been demonstrated by Striemer and Fauchet [102]. Essentially, the porosity is graded from very large at the surfaces to gradually from near 1 to the bulk value and reflection is efficiently suppressed.

A slightly exotic property of microporous Si may lead to special applications: it is highly explosive if kept under certain conditions [103,104]. First ideas for possible uses are expressed in the references given.

6. Experimental considerations

6.1. General

It is not uncommon that beginners in the field have initial problems to obtain homogeneous etching and reproducible results. Some factors that need attention are as follows.

- The back side contact of the sample may not be ohmic ("ohmic" meaning that the contact resistance shows a linear current voltage relationship and is small). Just putting Si on a metal plate is mostly not good enough, especially for low doped samples. Rubbing liquid In–Ga alloy on the back side, together with some scratching, usually will suffice. It is good practice to make two In-Ga spots and to measure the $I(V)$ characteristics between the spots. If it is linear, at least one of the contacts is ohmic.
- While reference electrodes are not always needed, it is usually advisable to use one in order to obtain reproducible results and to be relatively independent of the (temperature dependent) electrolyte conductivity. While a standard calomel electrode (SCE) is the reference electrode of choice for detailed measurements and experiments, a Pt wire may be sufficient for many practical cases including applications.
- A key issue is the addition of small amounts of surfactants to increase the "wetability" or to decrease surface tension effects, respectively. Common surfactants ("dish water detergents"), however, are not necessarily active in an acidic environment. The semiconductor industry routinely uses surfactants in its HF bathes which are commercially available (e.g. by Merck) and should be used. Exceptions are aqu electrolytes diluted with ethanol (which acts as wetting agent) and some org electrolytes for the same reason.
- Electrolyte flow is crucial for many experiments; it should be homogeneous and steady. This is not easily achieved with the commonly used peristaltic or membrane pumps. In some cases, the results of etching experiments depend sensitively on the pumping speed which then becomes a parameter to be controlled. A related problem are hydrogen bubbles which on occasion may cling to surface of the sample producing inactive spots and noise in the controlled parameter (usually the voltage or the light intensity). Bubbles must be avoided; pumping, surface reactants, and "sharp" seals at the edge of the sample help.
- All electrolytes dissolve some O_2 from the air which participates in the dissolution process. Since the oxidizing power of an electrolyte is one of its crucial characteristics, displacing dissolved O_2 by bubbling of the electrolyte with N_2 before use is often necessary for reproducible results.

- For many applications, especially if very perfect and deep pores are to be etched, control of the temperature is essential. Not only is it necessary to keep the temperature constant, room temperature is not always the best choice. A heat exchanger system, allowing temperature control between about 0 °C and 40 °C, should be part of an etching apparatus.
- If illumination is used, three additional problems arise: homogeneous and controllable illumination with a high intensity is needed, the backside contact must be at the edge of the sample for back side illumination, and the electrolytic cell must have a light transparent window for front side illumination.
- All materials in contact with the electrolyte must be chemically inert in this environment. For some electrolytes (especially, HF mixed with potent solvents like DMSO), this may limit the choice of materials to Teflon and its derivatives. Transparent windows, heat exchangers, etc. then are problematic and must be designed with care. Expensive sapphire windows and more Teflon have to be used. It is often a good idea to test a cell at first with inexpensive PVC and less aggressive electrolytes before the expensive final construction is made.
- While the electrolyte is primarily chosen from pore etching considerations, it is advisable to pay some attention to its conductivity and its pH value. The conductivity may be improved by adding salts to the solution, e.g. NH_4Cl to aqueous electrolytes with low HF concentration, or tetrabutylammonium-perclorate for MeCN, but for many organic electrolytes no suitable salts are known. Conducting salts, of course, may influence the etching in unpredictable ways, too. The pH value is mostly determined by the HF concentration, but it can be varied to some extent by the addition of acetic acid or by other means. There is, however, neither a strong indication that the pH value (for constant nominal HF concentration) is of prime importance for pore etching, nor much systematic investigation into this topic [58,105].

6.2. Large area etching

Most applications envisioned call for the etching of standard size Si wafers, at least 100 mm, better yet 150 or 200 mm. While any etching recipe that produces satisfying pores with small samples of typically 1–4 cm^2 will of course also work for larger wafers if the proper conditions can be maintained everywhere on the surface, there are a number of specific technical problems to large area etching that are not easy to solve. Etching n-macropores(bsi) is the most demanding task because of the necessary back side illumination. Problems encountered (and possible solutions) are as follows.

- The fraction j_{etch} of the hole current j_{photo} which is generated by illumination at the back side ($t = 0$) of a wafer with thickness d_w and a minority carrier diffusion length L that reaches the pore tips at a depth l as measured from the wafer surface is proportional to

$$\frac{j_{photo}}{j_{etch}} \propto \cosh\left(\frac{d_w - l}{L}\right) \approx \exp\left(\frac{d_w}{L}\right) \exp\left(-\frac{l}{L}\right). \tag{6.1}$$

In order to achieve a uniform and large current density for etching, the wafer thus should have a uniform and large diffusion length L and a "perfect" backside to minimize recombination losses at the back side. This is not automatically guaranteed with commercial n-type wafers, especially for larger doping concentrations.
- The light source must provide a homogeneous and intense coverage of the back side and must be controllable since for most applications the current is controlled by the light intensity. Arrays of light emitting diodes proved to be the best choice.

- The back side contact is very critical. If back side illumination is employed, it either can be supplied by a contact ring around the perimeter of the wafer (e.g. n^+ implantation and Al deposition through a mask followed by an anneal) which is expensive, by contact needles (necessarily damaging the Si) or by a (light transparent) electrolyte or ITO contact. While the Lehmann group favors contact needles, the group at Philips research uses an electrolyte contact [49]. Since a less aggressive electrolyte can be used for the contact, some of the problems encountered on the front side might be less severe for the backside contact in this case.
- While the current density is not very large (some $10 \, mA/cm^2$) the total current easily reaches 10 A. If contact problems exist, this may generate enough local heat to soften the polymers used for the cell, leading to leakage and serious safety problems.
- Besides removing the heat produced by ohmic losses, a constant temperature carefully adjusted to some optimum value (not necessarily around room temperature) is absolutely essential for successful etching and this requires large pumping and heat exchange equipment.
- The chemical reactions always release gases—mostly H_2—and for large wafers large amounts are produced which may lead to violent bubbling. An efficient means of safely removing the gases is necessary.
- Uniform pores will only result if the supply of reactants and the removal of products are homogeneous and stable. Circulation and/or movement of the electrolyte are mandatory and the flow pattern across the wafer must be either uniform in general, or uniform on time average.
- For making pre-structured n-macropores(aqu/bsi), usually an oxide mask is used. Pore etching commences at the openings of the mask and by the time the mask has dissolved the pores are deep enough for stable growth. Etching random pores, or pores through Si_3N_4 masks, may require an optimized nucleation step before the conditions for stable pore growth are established.
- While polished surfaces are not always necessary, it is a good idea to thoroughly clean the wafers if homogeneous random nucleation is desired, cf. Fig. 24.

Macropores on p-type Si—either in aqu or org electrolytes—do not require illumination which makes cell design easier (but with the added complexity of sever restrictions in useable materials). A design suitable for 150 mm wafers is now operative (after a year of optimization) in the Kiel group. Fig. 25 shows a schematic drawing.

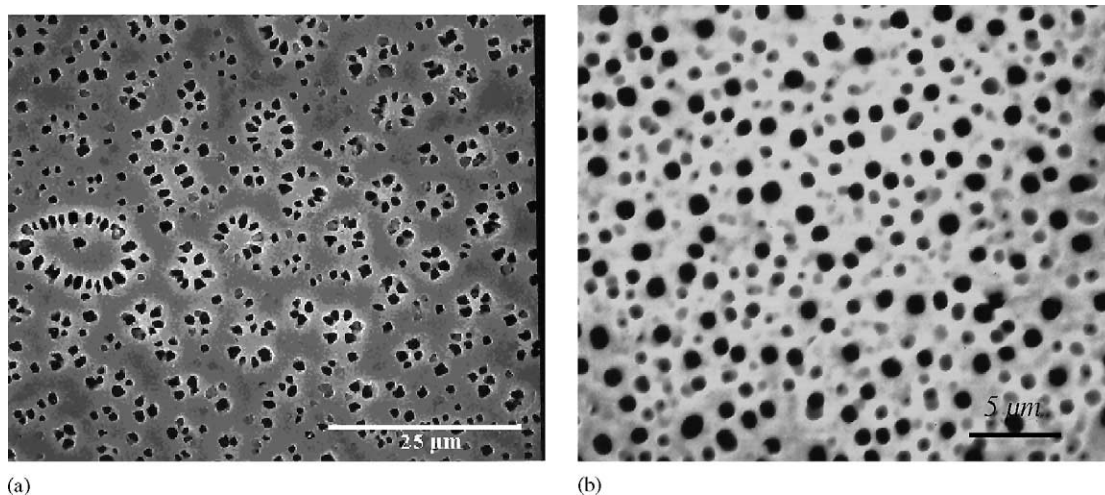(a)   (b)

Fig. 24. Random n-macropore(aqu/bsi) nucleated on (a) uncleaned and (b) cleaned samples.
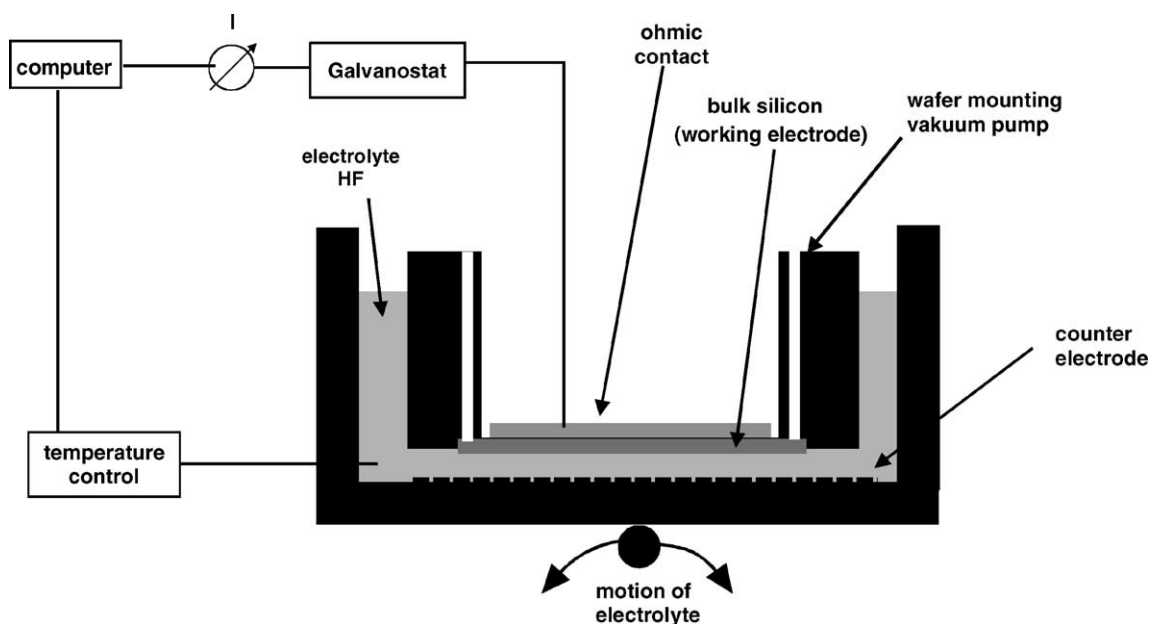
Fig. 25. Schematic drawing of the 150 mm cell developed for pore etching without illumination.

The cell has been constructed from PVC for the trial and error period which presently limits the use of organic electrolytes. So far, mostly p-macropores(aqu) were etched (p-macropores(org) (Fig. 26) have to await a reconstruction with Teflon only for the crucial parts. Fig. 25 shows some results demonstrating the homogeneity achieved.

Etching micro- and mesopores of just a few micrometers in depth on large areas is a comparatively easier task. Obviously the ELTRAN^{TM} [7] process has mastered this; but little is known about the cell design except that an electrolyte backside contact is used and several wafers are processed at the same time.

7. The current burst model

7.1. General features of the current burst model

A complete model of the electrochemistry of Si should not only be able to explain the bewildering multitudes of pores, but also the current or voltage oscillations and the peculiarities of the $I(V)$ characteristics. It must, moreover, accommodate the many models applicable to pore growth in some way, because those models are not wrong—SCR regions do exist and will focus holes on pore tips, avalanche break-through will occur at high field strength, and diffusion instabilities are real, too, as any snowflake or dendritic crystal will testify. Such a model then cannot be simple.

The current burst model (CBM) essentially claims to explain the electrochemistry of Si in the way defined above. It is an emerging model with many features not yet fully understood and some loose ends. Nevertheless, it explains current oscillations (at low frequencies) in a fully quantitative way [23,24], offers explanations in several issues of pore formation where all other models remain silent, and provides guidelines for the design of experiments and electrolytes (including III–V compounds) that have proved very useful in the investigations of the authors. In what follows we will
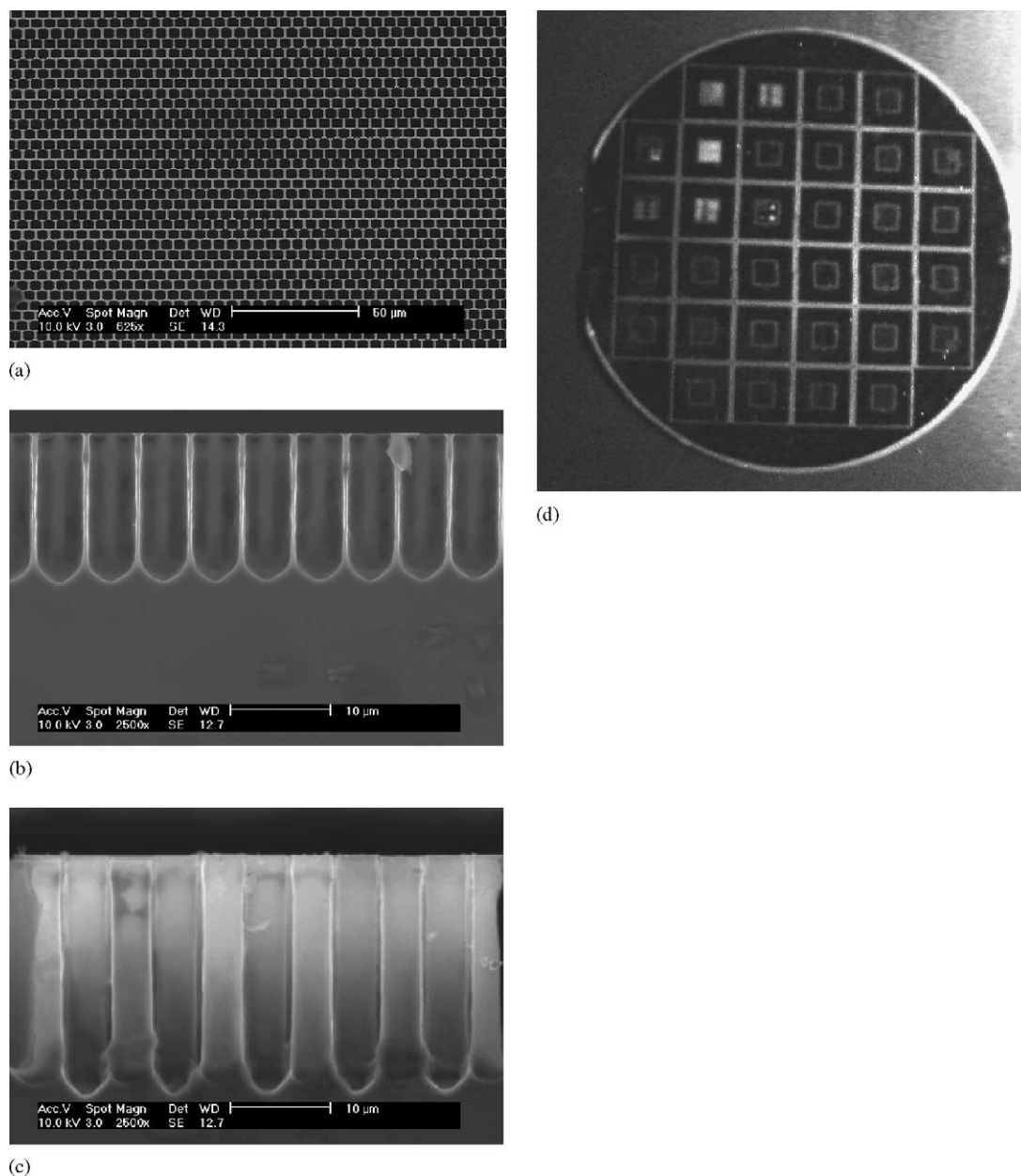
Fig. 26. The p-macropores(aqu) etched with the 150 mm cell from the center (a) plane view and two corners (b) and (c) with two different pitch sizes), respectively. (d) Luminescence light from a 150 mm wafer (exposed to UV light) with p-micropores(org/FA) etched through a nitride mask, demonstrating the homogeneity of the etching and, for the first time, micropores obtained with org electrolytes. Note that the structures in the quadrants are different.

present the salient features of the CBM without justification of single issues. For details, the reader is referred to [9,10,12,20].

When considering the electrochemistry of Si, it is always assumed (usually without even mentioning) that current flow is homogeneous in time and space. In other words, there is a well defined current density $j(x, y, t)$ on the electrode at any point in space and time which will only change smoothly from point to point. This, however, is intrinsically impossible for the following reasons.

Any electrochemical process that dissolves Si involves four distinctly different net chemical reactions.

1. *Direct dissolution* with the net reaction:

$$Si + xh^+ - ye^- \rightarrow Si^{4+}.$$
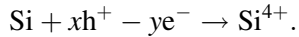
where x holes (h^+) are consumed in the reactions (and x must be ≥ 1), while y injected electrons (e^-) account for the rest of the charge needed. Direct dissolution thus makes the most efficient use of holes; it can proceed if only one hole is supplied.

2. *Oxidation* with the net reaction:

$$Si + 4h^+ + 2O^{2-} \rightarrow SiO_2.$$

Oxidation will always need four holes; it is thus not as efficient in the use of available holes as direct dissolution.

3. *Oxide dissolution* with the net reaction:

$$SiO_2 + 4F \rightarrow SiF_4 + O_2.$$
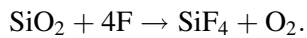
Oxide dissolution is a purely chemical process that does not need current flow or applied potentials. It essentially limits the total current that the system can process, because the oxide generation rate cannot be larger than the dissolution rate (on average).

4. *Hydrogen coverage* of the free Si surface, described by the formal (but useless) net reaction:

$$SiX + H \rightarrow SiH + X$$
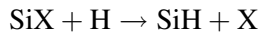
It means that whatever is sitting on the surface will be replaced by hydrogen in due time as given by some reaction constant k_{cov} as long as no other reactions take place. Far more important, however, than the simple coverage of the surface with hydrogen, is the concurrent removal (or *passivation*) of interface states having a certain density $\rho(E)$ in the band-gap of the Si which might also be described by first order reaction kinetics

$$\frac{d\rho(E)}{dt} = \rho_0 \exp(-k_{pas}t) \tag{7.1}$$

and k_{pas} = reaction constant = k_{pas} (orientation, chemistry, T). Note that k_{pas} is not identical to k_{cov}! In the CBM, the reaction constant k_{pas} plays a major role in pore formation and while it is generally not known, it is a measurable quantity.

Looking at a typical macropore growth situation, it is clear that both dissolution processes must occur simultaneously since the valence for the processes (i.e. the number of carriers flowing through the external circuit for one atom of Si dissolved) is usually around 2.7 and a single process should have an integer as valence. Oxide dissolution then is required, too, and, since the pore walls are obviously not carrying current, the H-passivation process must also be present. Obviously, the four processes cannot all occur at the *same* time *and* at the *same* place—totally homogeneous current flow is intrinsically impossible.

The problem could be swept under the rug by postulating that all processes occur at a very small scale with defined, but totally uncorrelated probabilities. Averaging over small, but not too small distances and times then would produce homogeneity in time and space, whereas inhomogeneities on a large-scale—as expressed in current oscillations and pores—could still be

possible. There is, however, no justification for this approach, even if that was the implicit hypotheses all along.

The current burst model goes to the other extreme and postulates that there are definite correlations between the four basic processes. It has three major postulates as follows.

1. Charge transfer and thus current flow is inherently inhomogeneous in time and space; in particular there are times when no charge is transferred in some areas at some time. A charge transfer process nucleates at (x, y, t) on the Si surface (or through a thin oxide) with a certain probability, p that depends on the surface "state" S at (x, y, t), but with an intrinsically stochastic probability element. The sequence of events started in this way is called a *current burst*.
2. The sequence of events in a current burst is dictated by logic. It must start with direct dissolution, followed by oxidation, followed by oxide dissolution, and, if a new current burst does not nucleate immediately, by hydrogen passivation. The lateral extension of a current burst is in the nm regime.
3. Individual current bursts may interact in space and time. This means that the nucleation probability, p of a current burst is not only a function of the surface state $S(x, y, t)$ but may depend on what has happened *before* at (x, y)—interaction in time—or on what is going on in the *neighborhood* at t—interaction in space. Assuming that the interaction in space and in time can be separated, we have

$$p(x, y, t) = \int\int_{x\pm\Delta x, y\pm\Delta y} d\tilde{x}\,d\tilde{y}\int_0^t d\tilde{t}\, W_r(x - \tilde{x}, y - \tilde{y}) \times W_t(t - \tilde{t}) \times S(\tilde{x}, \tilde{y}, \tilde{t}). \tag{7.1}$$

The essential parts are the functions W which contain the possible interactions in space and time and which will only be considered qualitatively in what follows. There are several ways in which current bursts can interact in space or time. First, we consider interaction in space.

One mechanism is described in detail in [23,24] and may be envisioned as follows: a current burst that nucleates between the oxide patches produced by two older ones has to produce less oxide before the field strength is low enough to stop oxidation. It interacts in space, but its behavior (the "switching off" and similarly, the "switching on") is correlated in time to its neighbors. *Interaction in space* thus results in a *correlation* in time, and if this interaction spreads by some percolation mechanism, areas of the electrode characterized in size by some correlation lengths L_{CO}, fire and quench their current bursts in (stochastic, i.e. never perfect) synchronization. This means that *domains* with a size given by L_{CO} are formed that erode the Si surface in a synchronized way.

Obviously, this interaction mechanism needs some minimum of oxidation, current densities not too low (so that current bursts have to nucleate in a density high enough to enable next neighbor interaction and some percolation), and oxide dissolution rates not too large. If the correlation length L_{CO} (a major quantity of the CBM) becomes comparable to the specimen size, macroscopic current oscillations will result [19]. Further interaction mechanisms are conceivable, but it does not matter for the essentials of the CBM exactly how interaction in space takes place.

Interaction in time is easy to visualize: if the nucleation probability p for a current burst depends on the potential or field strength at the interface, it will decrease with an increasing amount of passivation because passivation, as pointed out in Section 2.3, lowers the surface potential by allowing a space charge region to develop. Surfaces where no current bursts happened for some time are more passivated and thus less likely to nucleate a new CB. Turned around, CBs are more likely to nucleate where another CB took place not too long ago—there is an interaction in time. If strong enough, it will tend to cluster CBs in areas where other CBs were prominent—either because current was originally confined to some special places by using lithographically defined nucleation, or

because random fluctuations eventually cause precipitation of CBs. Since the kinetics of passivation are strongly anisotropic (cf. Section 2.3), so is CB nucleation, and CBs nucleate preferentially on {1 0 0} (and {1 1 3}) surfaces. *Interaction* in time thus leads to a *correlation* in space and CBs correlated in space are CB clusters which produce pores.

Pores with anisotropic behavior, under quite general circumstances, are thus a natural consequence of the CBM. Put in different words, stochastic interactions between localized events will under very general circumstances lead to a *phase separation* in the system: parts of the electrode contain many CBs and draw the highest current density possible under the circumstances, whereas other parts of the electrode are completely inert.

There are more types of correlations possible and the morphology (and to a lesser extent the geometry) of the pores can be linked to the dominating correlation.

- An ''anti correlation'' (meaning that the nucleation probability is highest wherever CBs have not happened before), together with quantum dot effects, produces micropores. This means that CB nucleate as soon as possible, i.e. right after oxide removal (most likely between some former bursts where the oxide was thinnest). This will draw a maximum of current because the active surface in this case will fold and thus is larger than the nominal surface. A sponge-like structure, not dependent on the crystal orientation, results with a porosity that increases with the current density—in other words we observe micropores.
- A positive interaction in time but without the formation of synchronized domains (or only very small domains), i.e. with no strong interaction in space, will produce mesopores. Current bursts eventually cluster and form pores with larger diameters. Avoidance of domains means insufficient oxidation and that can be seen as the common denominator of mesopores: they always form if the oxidation reaction is weak and direct dissolution is dominant. This may be induced by a lack of holes or weakly oxidizing electrolytes. Lack of holes is not an absolute measure but is defined relative to the amount of holes that electrolyte can process by direct dissolution. Increasing the doping of p-Si, e.g. increases the hole supply but because the potential at the interfaces increases too (less voltage drop in the SCR), the ability to use up holes in direct dissolution increases faster than the hole supply—in p^+ Si (and, in the same vein, n and n^+ Si in the dark) the oxidation reaction tends to be suppressed.
- Macropores form if sizeable domains are possible, i.e. if a minimum of oxidation permits interactions in space in addition to interaction in time. The morphology of the pores then is mainly determined by the mixture of length scales present. Only if the domain size and the other length scales (e.g. the SCR width in the case of n-macropores(aqu/bsi)) are close to each other, ''perfect'' macropores will result.

Before these somewhat abstract concepts will be applied to the more puzzling cases shown in the preceding chapters, some unique features of the CBM must be discussed. It does not only introduce an *intrinsic length scale* (the domain size L_{CO}), but also several *intrinsic time scales*. In particular, we have listed as follows.

- The average duration τ_{CB} of a CB. It is the sum of the average times for direct dissolution, oxidation, oxide dissolution and hydrogen passivation and determines directly the frequency of current or voltage oscillations. In many cases, the time for oxide dissolution will be the largest time in this sequence and a lower limit for τ_{CB} can than be obtained form the oxide dissolution kinetics.
- The average time τ_{DS} for the loss of synchronization between domains that started in phase. This is the mechanism that leads to damped current oscillations observed if the system is abruptly turned to some high voltage. The value of τ_{DS} can be considerably longer than τ_{CB}.

- The time τ_L it takes for a given pore to grow one correlation length L_{CO} into the depth of the sample. It has an important consequence: at least the time τ_L has to elapse before a (new) side pore can be dug into a pore wall by a domain of the size L_{CO}.

The CBM thus supplies intrinsic time scales and therefore the necessary ingredient for any kind of non-linear or resonant behavior if external time scales (e.g. the frequency of current modulations) are forced on the system.

7.2. The hammer model

For the case of macropores, the CBM can be expressed in a simple analogy, the "hammer model": macropores are formed by "hammering" them out of the silicon with a hammer that has the average size of a domain, i.e. L_{CO}. This hammer bangs away with the frequency $1/\tau_{CB}$ and every blow removes a patch of Si with a thickness corresponding to the average depth of a current burst. This is illustrated in Fig. 27.

The probability of a hammer strike is give by the nucleation probability of a current burst—the hammer will tend to strike on "soft" parts of the pore more often than on hard parts. At this stage, the correlations between current bursts are already part of the model (a pore has formed and a domain with defined size exists), the nucleation probability is now that of a whole domain. It depends, of course, on the carrier supply (CBs that nucleate but find no carriers will not "take") and on the passivation stage. Space charge regions, not containing carriers, thus are very hard, as are $\langle 1\,1\,1\rangle$ directions, while $\langle 1\,0\,0\rangle$ directions are "soft" and $\langle 1\,1\,3\rangle$ directions are not too hard, either.

We now can distinguish three basic cases: the hammer is smaller, larger, or comparable to the pore size (which might be determined by some of the other length scales of the system). This is shown in Fig. 28.

Case (a)—domain size larger than pore size—is obviously not possible! This explains why macropores with small diameters are so difficult to make—it is not only the width of the SCR that counts, but also the domain size.
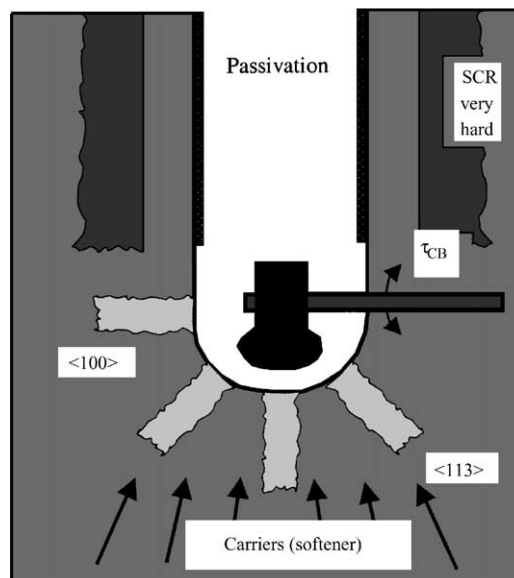

Fig. 27. The "hammer model". Silicon is always removed in patches corresponding to the domain size of the system.
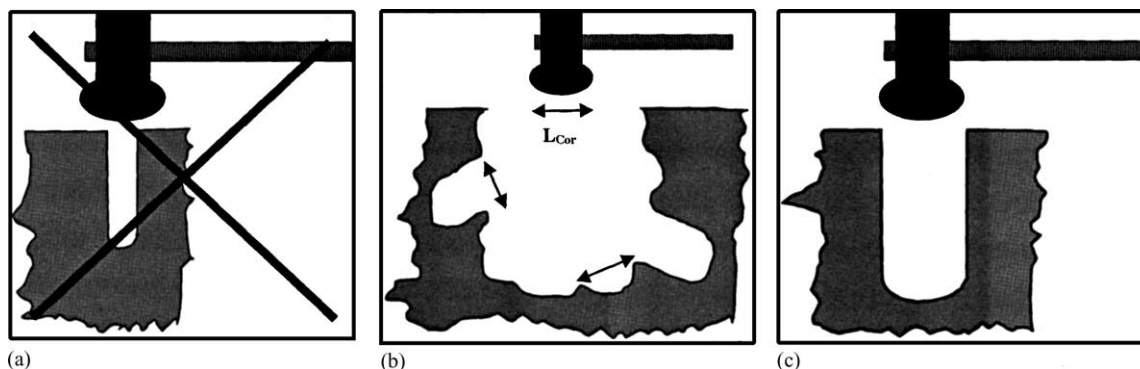
Fig. 28. Domain size and pore morphology. Case (a) is not possible; case (b) yields bulgy or branched pores and case (c) perfect pores.

Case (b)—making a large pore with one (or several) small hammers will produce rough pore wall or even branching. Note that the size of branches reflect the hammer size, and that a hammer, after striking off a side pore, will be trapped in this pore. It is also clear that a new side pore can only be formed if the main pore grew at least one hammer size into the depth and if that part of the pore wall is not sufficiently passivated yet.

Case (c)—simply gives "perfect pores". The hammer can only strike the bottom, each blow removes the same patch—the diameter is constant and no side pores are formed.

The simple hammer model explains easily most of the observations concerning all kinds of macropores. In particular, it is clear why very thin n-macropores(aqu/bsi) cannot be made and why the pores become very rough with increasing diameter (cf. Fig. 4). Very perfect pores mean that everything has to be just right. Changing parameters a little bit, e.g. the HF concentration from 4% where perfect n-macropores(aqu/bsi) result to, say 7% in order to increase the etch rate somewhat, will result in less perfect pores with rougher pore walls—as always observed.

The hammer model predicts exactly what is seen for the p-macropores(aqu) case shown in Fig. 10a and b. The natural size of the p-macropore(aqu) is given by the hammer size, the wall thickness corresponds to the SCR width. If the pores are forced to grow with larger diameters, the "hammers" become visible as bulges at the pore tip with dimensions identical to that of the size if randomly nucleated pores. Random nucleation, in this context, means that a domain stays in one area long enough (is "pinned") so that the proto-pore it produces effectively leads to self-pinning: the domain falls into the pit it dug itself!

The dependence of p-macropores(org) on the oxidizing power of the electrolyte and so on can be understood in principle, and, particularly interesting, the strange behavior of n-macropores(org/bsi) may be interpreted. Since the oxidation power of organic electrolytes is generally smaller than that of aqu electrolytes, it is reduced even more if the hole supply now is limited too, for n-type Si. The correlation length decreases—the hammer becomes smaller. We now have the case shown in Fig. 28b since the average pore distance is still dictated by SCR properties and the current flowing through the system thus must produce pores with diameters large than the hammer size.

Generally, side pores tend to form if a) one or a few small hammers must produce a big pore, and b) the H-passivation of the side walls is so slow that a hammer can still attack the side walls above the pore tip (then most likely the {1 0 0} or {1 1 3} surfaces oriented into the direction of hole supply). The second condition demands that the pore has-grown about one correlation length into the depth since the last branching in order to supply sufficient wall area. If these conditions are met,

three predictions emerge: (1) the diameter of the side pores is comparable to that of the main pore and given by the hammer size, i.e. the correlation length L_{CO}; (2) branches will be relatively regular and at a distance corresponding to the correlation length; (3) branching can be suppressed if the current density is periodically reduced with a frequency somewhat larger than $1/\tau_L$ with τ_L, as defined above = time to grow the pore a distance L_{CO} into the depth of the sample. This is to be expected because decreasing the current (which, at least under back side illumination conditions, always is focussed on the pore tip) forces the domains back to the pore tip and thus gives the side walls more time to passivate.

In summary, while the "hammer model" is certainly oversimplified, the general stochastic approach to electrochemistry of Si is not. While it still has loose ends and needs to be worked out in detail, it already supplies explanations of observed phenomena not obtainable in other models, predicts to a certain extent the outcome of experiments not yet performed, and, most valuable, gives concrete guidance for the design of electrolytes and experiments with a specific goal in mind.
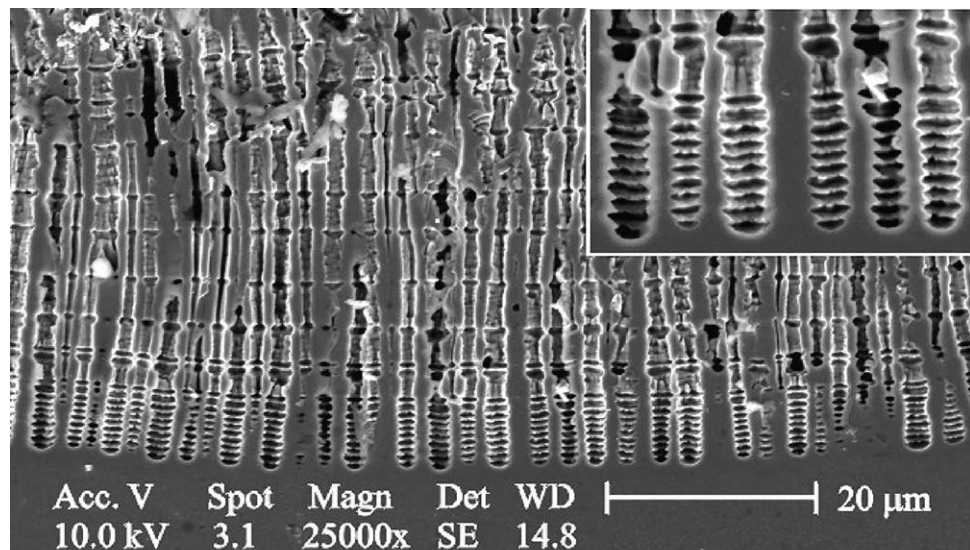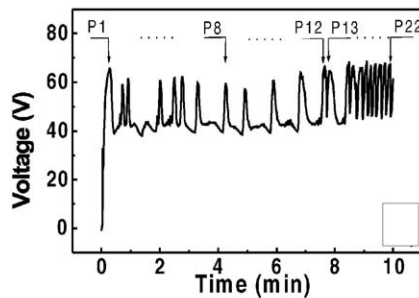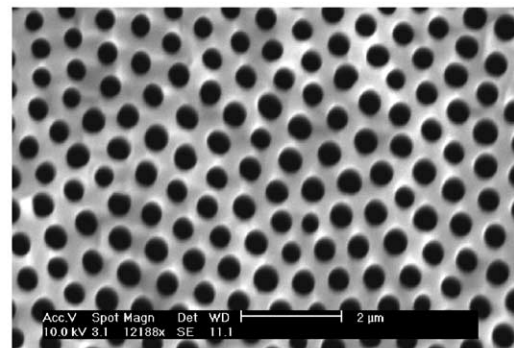
Fig. 29. Macropores in InP obtained in an HCl electrolyte (n-type, doping level = 1.5×10^{16} cm^{-3}, $j = 100$ mA/cm^2). (a) Macropores with periodic diameter oscillations, (b) voltage oscillations with peaks corresponding to the diameter oscillations, (c) top view showing tendency to form a hexagonal pore lattice (from [96]).

7.3. Pores in III–V compounds

It is possible to obtain electrochemically etched pores in III–V compounds, too, cf. [26–31]. In particular, pores in GaAs, GaP, and InP have been investigated, but much of the parameter space has not yet been systematically explored. While pores in these materials are often very different in their general appearance from pores in Si, there are some similarities, too.

A particular interesting feature is that while current or voltage oscillations akin to those in Si in the electropolishing regime have not been observed, voltage oscillations have recently been found to occur during macropore etching in all three materials mentioned [106], Fig. 29 shows some examples.

Similar results have been obtained in GaP and GaAs samples. The CBM maintains that the stochastic processes governing current and voltage oscillations in Si are essentially also responsible for pore formation in other semiconductors. Macroscopic oscillations and pore formation, however, have never been observed together in Si. Their occurrence in III–V compounds, nevertheless, adds credibility to basic assumptions of the CBM; a detailed analysis, however, will transgress the intentions of this paper and will be published elsewhere.

References

[1] L.T. Canham, J. Appl. Phys. Lett. 57 (1990) 1046.
[2] V. Lehmann, U. Gösele, J. Appl. Phys. Lett. 58 (1991) 856.
[3] V. Parkhutik, Solid State Electron. 43 (1999) 1121–1141.
[4] M.P. Stewart, J.M. Buriak, Adv. Mater. 12 (2000) 859.
[5] M.J. Sailor, Sensor application of porous silicon, in: L.T. Canham (Ed.), Properties of Porous Silicon, IEE-Books, London, 1997.
[6] L.T. Canham, Biomedical applications of porous silicon, in: L.T. Canham (Ed.), Properties of Porous Silicon, IEE-Books, London, 1997.
[7] T. Yonehara, BESOI with porous silicon: ELTRAN, in: L.T. Canham (Ed.), Properties of Porous Silicon, IEE-Books, London, 1997.
[8] M.G. Berger, M. Thönissen, W. Theiß, H. Münder, Microoptical devices based on porous silicon, in: M.O. Manasreh (Ed.), Optoelectronical Properties of Semiconductors and Superlattices, vol. 5, Gordon and Breach, Amsterdam, 1997.
[9] J. Carstensen, M. Christophersen, H. Föll, Mater. Sci. Eng. B 69/70 (2000) 23.
[10] J. Carstensen, M. Christophersen, G. Hasse, H. Föll, Phys. Stat. Sol. (a) 182 (2000) 63.
[11] G. Hasse, J. Carstensen, G.S. Popkirov, H. Föll, Mater. Sci. Eng. B 69/70 (2000) 188.
[12] H. Föll, J. Carstensen, M. Christophersen, G. Hasse, Phys. Solid State (a) 182 (2000) 7.
[13] H. Föll, V. Lehmann, European Patent EP0400387B1 (1990).
[14] E. Yablonovitch, D.L. Allara, C.C. Chang, T. Gmitter, T.B. Bright, Phys. Rev. Lett. 57 (1986) 249.
[15] V. Lehmann, H. Föll, J. Electrochem. Soc. 135 (1988) 2831.
[16] J. Carstensen, W. Lippik, H. Föll, in: H.R. Huff, W. Bergholz, K. Sumino (Eds.), Semiconductor Silicon/1994 (ECS Proc. Vol. 94-10), San Francisco, 1994, p. 1105.

[17] H. Föll, J. Appl. Phys. 53A (1991) 8.
[18] G. Mende, E. Hensel, Thin Solid Films 168 (1989) 51.
[19] G. Hasse, J. Carstensen, H. Föll, in: P. Schmuki, D.J. Lockwood, Y.H. Ogata, H.S. Isaacs (Eds.), ECS Proceedings, 2001, submitted for publication.
[20] H. Föll, J. Carstensen, M. Christophersen, G. Hasse, in: P. Schmuki, D.J. Lockwood, Y.H. Ogata, H.S. Isaacs (Eds.), Pits and Pores II: Formation Properties and Significant for Advanced Materials, Electrochemical Society Meeting Proceedings, 2001, p. 36.
[21] S. Rönnebeck, J. Carstensen, S. Ottow, H. Föll, Electrochem. Solid State Lett. 2 (1999) 126.
[22] M. Christophersen, J. Carstensen, A. Feuerhake, H. Föll, Mater. Sci. Eng. B 6970 (2000) 194.
[23] J. Carstensen, R. Prange, H. Föll, J. Electrochem. Soc. 146 (1999) 1134.
[24] J. Carstensen, R. Prange, G.S. Popkirov, H. Föll, J. Appl. Phys. A 67 (1998) 459.
[25] O. Jessensky, F. Müller, U. Gösele, J. Electrochem. Soc. 145 (1998) 3735.
[26] P. Schmuki, J. Fraser, C.M. Vitus, M.J. Graham, J. Electrochem. Soc. 143 (1996) 3316–3322.
[27] S. Langa, J. Carstensen, M. Christophersen, H. Föll, I.M. Tiginyanu, J. Appl. Phys. Lett. 78 (2001) 1074–1076.
[28] B.H. Erne, D. Vanmaekelbergh, J.J. Kelly, J. Electrochem. Soc. 143 (1996) 305–314.
[29] M.A. Stevens-Kalceff, S. Langa, I.M. Tiginyanu, J. Carstensen, M. Christophersen, H. Föll, in: P.M. Fauchet, J.M. Buriak, L.T. Canham, N. Koshida, B.E. White Jr. (Eds.), Microcrystalline and Nanocrystalline Semiconductors. Mater. Res. Soc. Symp. Proc. (638) 2000.
[30] T. Takizawa, S. Arai, Jpn. J. Appl. Phys. 54 (1994) L643.
[31] S. Langa, I.M. Tiginyanu, J. Carstensen, M. Christophersen, H. Föll, J. Electrochem. Solid State Lett. 3 (2000) 514.
[32] V.P. Parkhutik, E. Matveeva, Electrochem. Solid State Lett. 2 (1999) 371.
[33] E.K. Propst, P.A. Kohl, J. Electrochem. Soc. 141 (1994) 1006.
[34] M. Christophersen, J. Carstensen, H. Föll, Phys. Stat. Sol. (a) 182 (2000) 45.
[35] V. Lehmann, H. Föll, J. Electrochem. Soc. 137 (1990) 653.
[36] V. Lehmann, J. Electrochem. Soc. 140 (1993) 2836.
[37] V. Lehmann, W. Hönlein, H. Reisinger, A. Spitzer, H. Wendt, J. Willer, Solid State Technol. 38 (1995) 99.
[38] V. Lehmann, U. Grüning, Thin Solid Films 297 (1997) 13–17.
[39] M. Hejjo Al Rifai, M. Christophersen, S. Ottow, J. Carstensen, H. Föll, J. Electrochem. Soc. 147 (2000) 627.
[40] M.J.J. Theunissen, J. Electrochem. Soc. 119 (1972) 351.
[41] V. Lehmann, S. Stengl, A. Luigart, Mater. Sci. Eng. B 69/70 (2000) 11.
[42] J.-N. Chazalviel, R. Wehrspohn, F. Ozanam, Mater. Sci. Eng. B 69/70 (2000) 1.
[43] R.L. Smith, S.D. Collins, J. Appl. Phys. 71 (1992) R1.
[44] V. Lehmann, U. Gösele, Adv. Mater. 4 (1992) 114.
[45] F. Müller, A. Birner, J. Schilling, R.B. Wehrspohn, U. Gösele, Adv. Solid State Phys. 40 (2000) 545.
[46] U. Grüning, Ph.D. Thesis, Erlangen, 1997.
[47] P. Kleinmann, J. Linnros, S. Petersson, Mater. Sci. Eng. B 69/70 (2000) 29.
[48] F. Müller, A. Birner, J. Schilling, U. Gösele, C. Kettler, P. Hänggi, Phys. Stat. Sol. (a) 182 (2000) 585.
[49] J.E.A.M. van den Meerakker, R.J.G. Elfrink, F. Roozeboom, J.F.C.M. Verhoeven, J. Electrochem. Soc. 147 (2000) 2757.
[50] M. Christophersen, P. Merz, J. Quenzer, J. Carstensen, H. Föll, Sens. Actuators A 88 (2001) 241.
[51] M. Christophersen, J. Carstensen, H. Föll, Phys. Stat. Sol. (a) 182 (2000) 601.
[52] M.M. Rieger, P.A. Kohl, J. Electrochem. Soc. 142 (1995) 1490.
[53] E.A. Ponomarev, C. Levy-Clement, J. Electrochem. Soc. Lett. 1 (1998) 1002.
[54] M. Christophersen, J. Carstensen, H. Föll, Phys. Stat. Sol. (a) 182 (2000) 103.
[55] H. Ohji, P.J. French, K. Tsutsumi, Sens. Actuators A 82 (2000) 254.
[56] K.J. Chao, S.C. Kao, C.M. Yang, M.S. Hseu, T.G. Tsai, Electrochem. Solid State Lett. 3 (2000) 489.
[57] C. Levy-Clement, A. Lagoubi, M. Tomkiewicz, J. Electrochem. Soc. 141 (1971) 958.
[58] R.L. Meek, Surf. Sci. 25 (1971) 526.
[59] A. Valance, Phys. Rev. B 52 (1995) 8323.
[60] V. Lehmann, S. Rönnebeck, J. Electrochem. Soc. 146 (1999) 2968.
[61] V. Lehmann, R. Stengl, A. Luigart, Mater. Sci. Eng. B 69/70 (2000) 11.
[62] S. Ottow, V. Lehmann, H. Föll, J. Electrochem. Soc. 143 (1996) 385.
[63] S. Ottow, V. Lehmann, H. Föll, Appl. Phys. A 63 (1996) 153.
[64] J. Rousselet, L. Salomone, A. Ajdari, J. Proust, Nature 370 (1994) 446.
[65] C. Kettner, P. Reimann, P. Hänggi, F. Müller, Phys. Rev. E 61 (2000) 212.
[66] V. Lehmann, S. Rönnebeck, Sens. Actuators A 95 (2001) 202.
[67] M. Bengtsson, S. Ekstöm, J. Drott, A. Collins, E. Csöregi, G. Marko-Varga, T. Laurell, Phys. Stat. Sol. 182 (2000) 495.
[68] V. Lehmann, S. Ottow, R. Stengl, H. Reisinger, H. Wendt, European Patent WO9961147 (1999).
[69] V. Lehmann, Electrochemistry of Silicon, Wiley-VCH, Weinheim, 2002.
[70] R. Angelucci, A. Poggi, L. Dori, A. Tagliani, G.C. Cardinali, F. Corticelli, M. Madisaldi, J. Porous Mater. 7 (2000) 197.
[71] E.V. Astrova, V.B. Voronkov, I.V. Grekov, Tech. Phys. Lett. 25 (1999) 958.
[72] H. Föll, V. Lehmann, European Patent EP0296348B1 (1993).

[73] V.V. Starkov, E.Y. Gavrilin, J. Konle, H. Presting, A.F. Vyatkin, U. König, Phys. Stat. Sol. (a), 2000, in press.
[74] H. Föll, J. Grabmaier, V. Lehmann, German Patent DE 3324232 C2 (1983).
[75] A. Prasad, S. Balakrishnan, S.K. Jain, G.C. John, J. Electrochem. Soc. 129 (1982) 596.
[76] M. Liponski, P. Panek, S. Bastide, C. Levy-Clement, Phys. Stat. Sol. (a), 2002, in press.
[77] E.A. Ponomarev, C. Levy-Clement, J. Porous Mater. 7 (2000) 51.
[78] S.R. Nicewarner-Pena, R.G. Freeman, B.D. Reiss, L. He, D.J. Pena, I.D. Walton, R. Cromer, C.D. Keating, M.J. Natan, Science 294 (2001) 137.
[79] E. Yablonovitch, Phys. Rev. Lett. 58 (1987) 2059.
[80] S. John, Phys. Rev. Lett. 58 (1987) 2486.
[81] U. Grüning, S. Ottow, V. Lehmann, Appl. Phys. Lett. 68 (1996) 747.
[82] A. Birner, K. Busch, F. Müller, Phys. Biol. 55 (1999) 27.
[83] F. Müller, A. Birner, U. Gösele, V. Lehmann, S. Ottow, H. Föll, J. Porous Mater. 7 (2000) 201.
[84] V. Lehmann, R. Stengl, H. Reisinger, R. Detempele, W. Theiss, Appl. Phys. Lett. 78 (2001) 589.
[85] P. Merz, German Patent DE 199,56,654 A1 (1999).
[86] C. Jäger, B. Finkenberger, W. Jäger, M. Christophersen, J. Carstensen, H. Föll, Mater. Sci. Eng. B 69/70 (2000) 199.
[87] R.B. Bergmann, T.J. Rinke, J.H. Werner, Phys. Biol. 56 (2000) 51.
[88] R. Brendel, R. Auer, Phys. Stat. Sol. (a), 2002, in press.
[89] K. Sakaguchi, H. Kurisu, K. Ohmi, T. Yonahara, in: P. Schmuki, D.J. Lockwood, Y.H. Ogata, H.S. Isaacs (Eds.), ECS Proceedings, 2001, in press.
[90] K. Imai, H. Unno, IEEE Trans. Electron Devices 31 (1984) 297.
[91] W. Lang, in: M.O. Manasreh (Ed.), Optoelectronical Properties of Semiconductors and Superlattices, vol. 5, Gordon and Breach, Amsterdam, 1997.
[92] N. Koshida, H. Koyam, Appl. Phys. Lett. 60 (1992) 347.
[93] J. Buriak, M. Allen, J. Lumin. 80 (1999) 29.
[94] M. Thönissen, S. Billat, U. Frotscher, U. Rossow, M. Krüger, H. Tüth, M.G. Berger, J. Appl. Phys. 80 (1996) 2990.
[95] G. Lérondel, T. Yao, in: proceedings of the PSST Conference (extended abstracts), 2000, p. 138.
[96] J.M. Buriak, Adv. Mater. 11 (1999) 265.
[97] S. Letant, M.J. Sailor, Adv. Mater. 12 (2000) 355.
[98] W. Lang, Mater. Sci. Eng. R17 (1996) 1–55.
[99] L.T. Canham, Adv. Mater. 7 (1995) 1033.
[100] A.H. Mayne, S.C. Bayliss, P. Barr, M. Tobin, L.D. Backberry, Phys. Stat. Sol. 182 (2000) 505.
[101] L.T. Canham, R. Aston, J.-N. Chazalviel, C. Reeves, Phys. Stat. Sol. (a), 2002, in press.
[102] C.C. Striemer, F. Fauchet, Phys. Stat. Sol. (a), 2002, in press.
[103] D. Kovalev, V.Yu. Timoshenko, N. Künzner, E. Gross, F. Koch, Phys. Rev. Lett. 87 (2001) 068301.
[104] B.E. Collins, K.-P.S. Dancil, G. Abbi, M.J. Sailor, Adv. Funct. Mater. 12 (2002) 187.
[105] J.-N. Chazalviel, in: J.-C. Vial, J. Derrien (Eds.), Porous Silicon Science and Technology, Springer, Berlin, 1995, p. 17.
[106] S. Langa, J. Carstensen, I.M. Tiginyanu, M. Christophersen, H. Föll, Electrochem. Solid State Lett. 4 (2001) G50.